Appl Biochem Biotechnol (2009) 157:174–209
DOI 10.1007/s12010-008-8279-z

Structure and Action Mechanism of Ligninolytic Enzymes

Dominic W. S. Wong

Received: 8 February 2008 / Accepted: 5 May 2008 /
Published online: 26 June 2008

Abstract Lignin is the most abundant renewable source of aromatic polymer in nature, and its decomposition is indispensable for carbon recycling. It is chemically recalcitrant to breakdown by most organisms because of the complex, heterogeneous structure. The white-rot fungi produce an array of extracellular oxidative enzymes that synergistically and efficiently degrade lignin. The major groups of ligninolytic enzymes include lignin peroxidases, manganese peroxidases, versatile peroxidases, and laccases. The peroxidases are heme-containing enzymes with catalytic cycles that involve the activation by H_2O_2 and substrate reduction of compound I and compound II intermediates. Lignin peroxidases have the unique ability to catalyze oxidative cleavage of C–C bonds and ether (C–O–C) bonds in non-phenolic aromatic substrates of high redox potential. Manganese peroxidases oxidize Mn(II) to Mn(III), which facilitates the degradation of phenolic compounds or, in turn, oxidizes a second mediator for the breakdown of non-phenolic compounds. Versatile peroxidases are hybrids of lignin peroxidase and manganese peroxidase with a bifunctional characteristic. Laccases are multi-copper-containing proteins that catalyze the oxidation of phenolic substrates with concomitant reduction of molecular oxygen to water. This review covers the chemical nature of lignin substrates and focuses on the biochemical properties, molecular structures, reaction mechanisms, and related structures/functions of these enzymes.

Keywords Lignin peroxidase · Manganese peroxidase · Versatile peroxidase · Laccase · Lignin degradation

Reference to a company and/or products is only for purposes of information and does not imply approval of recommendation of the product to the exclusion of others that may also be suitable. All programs and services of the US Department of Agriculture are offered on a nondiscriminatory basis without regard to race, color, national origin, religion, sex, age, marital status, or handicap.

D. W. S. Wong (✉)
Western Regional Research Center, USDA-ARS, 800 Buchanan Street, Albany, CA 94710, USA
e-mail: dwsw@pw.usda.gov

Chemistry of Lignin Structure

Lignin is found in all vascular plants, representing an abundant carbon source on earth, second only to cellulose. The term "lignin" has its origin in the Latin word "lignum" which means wood. Lignin is extremely recalcitrant to degradation, with a complex structure derived from oxidative-coupling of monolignols (lignin monomers, monomeric precursors), the three primary hydroxycinnamyl alcohols: *p*-coumaryl, coniferyl, and sinapyl alcohols. The corresponding phenylpropanoid units in the lignin polymer (known as lignin polymer units) are denoted as *p*-hydrophenyl (*H*), guaiacyl (*G*), and syringyl (*S*) units, respectively, based on the methoxy substitution on the aromatic rings (Fig. 1). Softwood (gymnosperms, conifers such as spruce, cedar, and hemlock) lignin, in general, contains mostly *G* units and very low levels of *H* units (*G*/*S*/*H*=96:*t*:4). Hardwood (angiosperms, leafy deciduous trees such as poplar, willow, birch, and alder) lignin is comprised of similar levels of *G* and *S* units with traces of *H* units (*G*/*S*/*H*=50:50:*t*). Grasses (monocots) contain all three with *G*/*S*/*H*=70:25:5 [1–3]. It should be noted that these ratios are meant for generalities in very simply terms, because compositional variations among species and structural heterogeneity of lignin within plants are well documented.

Lignification is achieved by cross-linking reactions of a monomer with the growing polymer or by polymer–polymer coupling via radicals generated by oxidase enzymes. Because of resonance delocalization of radicals to couple at various sites, an array of structural units formed by ether and C–C linkages is found in the resulting polymer. These include β-*O*-4, β-5, β-β, 5-5, 4-*O*-5, and β-1 couplings (Fig. 2). Acylated structural units, such as 4-propoxy-sinapyl-γ-acetate, are found at high levels in "kenaf" lignin and recently in other lignins. Hydroxycinnamic acids esterified at the γ-position of the propyl side chains of lignin and also as end groups are present in grasses [4, 5]. Endwise reactions

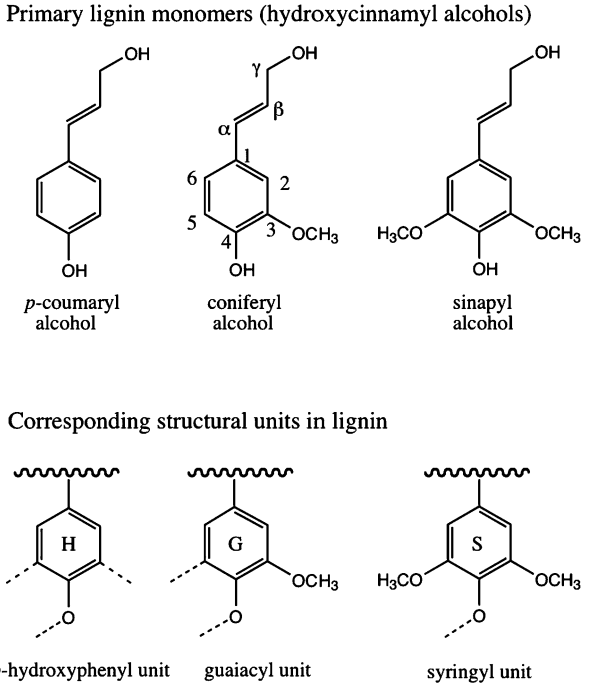

Fig. 1 Primary lignin monomers and corresponding lignin units

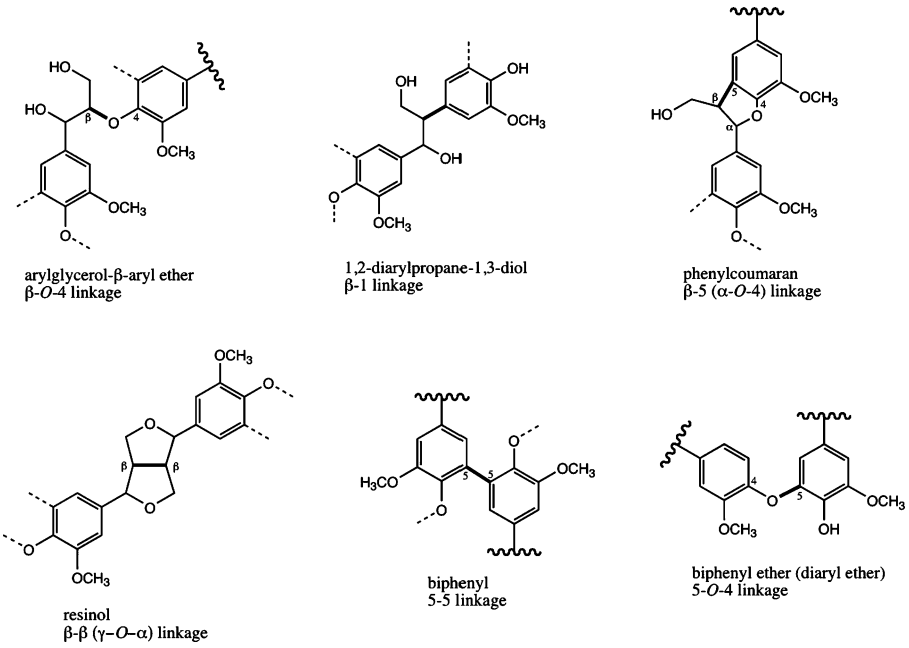

Fig. 2 Major structural units derived from cross-coupling of monomers

coupling a monomer (usually a monolignol at its β-position) to the growing polymer give rise to β-linked structures. Coupling between two preformed lignin oligomers or polymers results in 5-5 and 5-*O*-4 linked structures. The coupling of two monomers (dimerization) to yield β-β (resinol) structures is only a minor event in nature, although it occurs frequently in synthetic lignin synthesis. End groups arise from coupling reactions that are not at the side chain β-position of the monomer. The relative abundance of the different linkages largely depends on the relative contribution of the monomers to the polymerization process during lignin biosynthesis. Coupling of a monolignol, for example, coniferyl alcohol, to a G unit in a growing lignin oligomer/polymer, yields G-β-*O*-4-G and G-β-5-G linkages (Fig. 3), while cross-coupling of G units from two growing lignin oligomer/polymer results in G-5-5-G and G-4-*O*-5-G linkages (Fig. 4). However, coupling of a coniferyl alcohol to an S unit yields only G-β-*O*-4-S, but not G-β-5-S, because coniferyl alcohol has a methoxy group at the 5 position. Likewise, cross-coupling of G and S units from two growing lignin oligomer/polymer results in S-4-*O*-5-G linkage, but not 5-5 linkage, and also two S units will not give coupling products. The β-*O*-4 (arylglycerol-β-aryl ether) coupling of a monolignol with the growing lignin oligomer/polymer creates the most abundant structural unit, involving generally ~50% and 80% of the phenylpropanoid units in softwood and in hardwood lignin, respectively [6]. The β-5, 5-5, and 4-*O*-5 structures account for ~10%, 25%, and 4%, respectively, in softwood lignin [1]. The amount of β-1 structures in softwood lignin is about 2% [6]. However, cautions should be taken with these generalities because exceptions to these ratio trends occur. The β-*O*-4 bond is easily cleaved chemically during delignification (pulping) process, while C–C, styryl ether, and biphenyl ether bonds are resistant to solvolytic chemical degradation. The 5-5 unit is frequently etherified with additional monolignol via intramolecular reaction of quinone methide intermediates [7, 8]. The resulting dibenzodioxocin, an eight-member cyclic ether unit, as well as the 5-5 and 4-*O*-5 units may serve as branching points in softwood lignin. Similarly, some β-

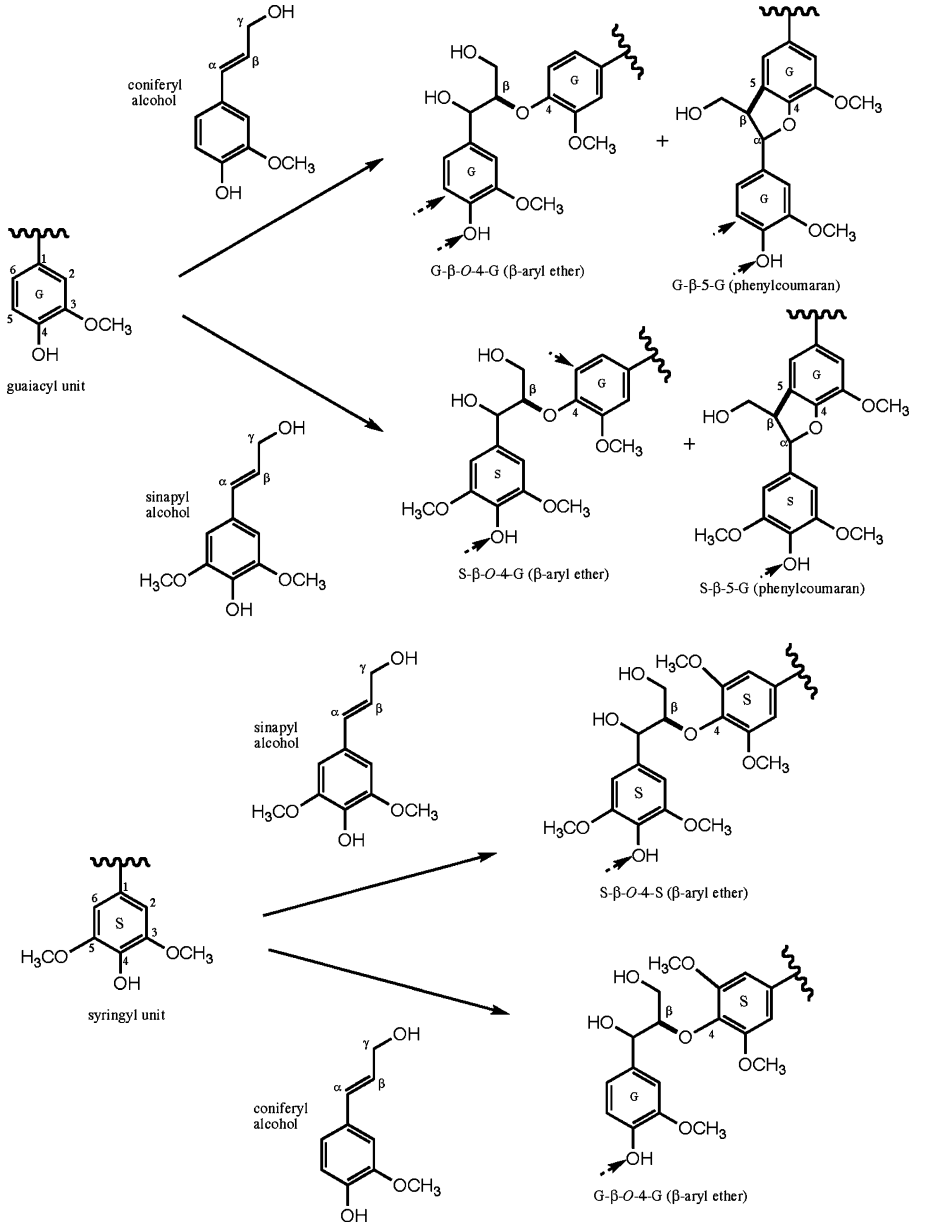

Fig. 3 Structural units derived from endwise coupling

1-linkages seem to be part of spirodienone substructures recently identified in lignin using two-dimensional nuclear magnetic resonance [9].

Over the years, various hypothetical models of lignin molecular structures have been proposed based on the random coupling theory, and available data on the types and distributions of inter-units and linkages, using an arbitrary number of units. The actual lignin structure is very complex, and existing lignin models neither imply any particular sequence of monomeric units nor reflect the actual network of monomers in the lignin

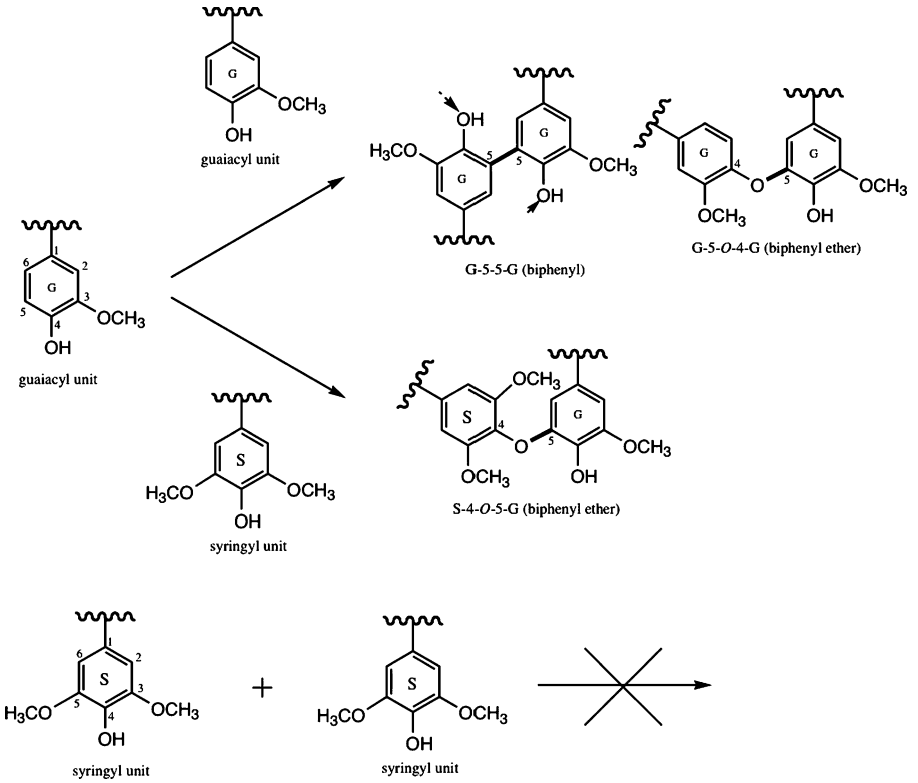

Fig. 4 Structural units derived from polymer–polymer coupling

macromolecule. Details on how the polymerization process is controlled in the plant have not been completely established. The coupling model in which the monolignols react endwise with the growing polymer under simple chemical control produces random linkages and hence a lignin structure that is not absolutely defined or determined [10]. On the other hand, the template replication model proposed in recent years, but still lacking experimental demonstration, suggests that bond formation in lignin polymerization is under biochemical control. Endwise polymerization is guided by proteinaceous sites on a template that stipulate linkage types and configurations [11, 12].

Lignin Preparations

A major obstacle in elucidating lignin structure has been the isolation of native, highly representative, and totally unaltered lignin from wood. Brauns' lignin, often referred to as native lignin in early literature, is isolated by extraction of ground wood (sawdust particle size) with 95% ethanol at room temperature. The crude lignin in the extract is purified by repeated precipitation from its solution in dioxane into ether [13, 14]. The preparation has a low yield of ~8% of the total lignin and contains mostly low molecular weight lignins.

The more useful lignin preparation is "milled wood lignin" (MWL) isolated by the method of [15]. Although variations in the conditions exist, the basic procedure involves ball milling of the ground wood to produce very fine powder wood meal for extraction of

lignin using neutral solvent systems, such as dioxane. Lignin is precipitated from the extract as milled wood lignin using various solvents. MWL is generally considered representative of the total lignin in the wood and widely used for chemical and biological investigations, although it has been well documented that the MWL isolation procedure causes depolymerization and modification of the lignin in addition to its low yield of about 20–30% [16]. A modification of the Bjorkman method involves extraction of lignin by dioxane–water acidified with HCl to yield acidolysis dioxane lignin. The main advantages of acidolysis are shorter reaction time and higher yield, but linkage breakdown and condensation reactions occur considerably with increasing temperature and acidity [17].

Wood meal may be treated with cellulolytic/hemicellulolytic enzymes to remove majority of the polysaccharides [18]. The insoluble residue after enzyme treatment is referred to as milled wood enzyme lignin (MWEL). MWEL is considered a close representation of the native lignin, with higher yields as much as 95% and fewer chemical changes than in MWL, but contains undesirably high (10–12%) carbohydrate contents. The procedures for MWL and MWEL can be combined by treating the wood meal with enzymes to release the carbohydrates, followed by extraction of the insoluble material with dioxane–water to solubilize the lignin [8, 19]. The product is referred to as cellulolytic enzyme lignin (CEL).

Synthetic lignins, often referred to as "dehydrogenative polymerizate" (DHP), are prepared by separate and simultaneous addition of coniferyl alcohol and/or other monolignols, and H_2O_2 to a buffered solution of peroxidase. Synthetic lignin can be ^{14}C-labeled at the β- and γ-carbons of the side chain, in the methoxy groups or in the aromatic ring carbons. The ^{14}C-labeled lignin is a widely used substrate for quantitative investigation of lignin degradation by measuring the evolution of labeled carbon dioxide [20, 21]. Both DHP and labeled lignin are used extensively for studies of biological modification and degradation, as well as for chemical characterization.

Industrial lignins or technical lignins refer to lignins recovered as by-products from chemical pulping, as well as from other biomass-based processes. These lignins have undergone extensive depolymerization, chemical modification, and structural changes. In acid sulfite pulping, wood chips are treated with a hot acid solution of calcium hydrogen sulfite, $Ca(HSO_3)_2$. The process results in sulfonation and dissolution of the lignin and formation of lignosulfonates (hence, called sulfite lignin) in the sulfite liquor. The vast majority of chemical pulp produced worldwide is generated by alkaline kraft pulping, in which wood chips are treated with NaOH and Na_2S at high temperatures. The lignin is recovered from the spent (black) liquor as a brown insoluble material, referred to as kraft lignin (sulfate lignin). Organosolv lignins are produced from different organic solvent-based systems, such as ethanol/water or acetic acid/HCl pulping, and contain a more oxidized structure.

Lignin-Degrading Fungi

Lignin resists attack by most microorganisms; anaerobic processes tend not to attack the aromatic rings at all, and aerobic breakdown of lignin is slow. In nature, only basidiomyceteous white-rot fungi are able to degrade lignin efficiently, where solubilization (formation of water soluble fragments) and minineralization (evolution of CO_2 as determined by ^{14}C-labeling) of natural and synthetic lignins have been demonstrated [20, 22]. Wood decayed by white rot fungi is pale in color because of oxidative bleaching and loss of lignin and often retains a fibrous texture. Some white-rot fungi preferentially attack

lignin more readily than hemicellulose and cellulose in the wood tissue [23–25]. This process of selective delignification leaves enriched cellulose, as observed in the white regions of a mottled rot and in the pockets of a white pocket rot. There is considerable interest in the industrial application of these fungi, because many uses of wood involve preferentially removing lignin, such as in biopulping. *Ceriporiopsis subvermispora*, *Phellimus pini*, *Phlebia* spp., and *Pleurotus* spp. belong to this fungi group. Many white-rot fungi, however, exhibit a pattern of simultaneous decay characterized by degradation of all cell wall components with formation of radial cavities. Examples of this group of fungi include *Trametes versicolor*, *Heterobasidium annosum*, and *Irpex lacteus* [26, 27].

In contrast to white-rot fungi, which are more commonly found on deciduous (angiosperms) wood, brown-rot fungi grow primarily on conifers (gymnosperms) and represent 7% of wood-rotting basidiomycetes [28]. Brown-rot fungi degrade wood carbohydrates, resulting in typically brown-colored rot because of the oxidized lignin left behind [29]. The decayed wood shows a cross-checking texture with cracks and clefts because of the loss of cellulose, a phenomenon hence referred to as "cubical" brown rot. Examples of this group of fungi include *Gloeophyllum trabeum*, *Laetiporus portentosus*, *Fomitopsis lilacino-gilva*, *Piptoporus betulinus*, *Postia placenta*, and *Serpula lacrimans*.

Ligninolytic Enzymes

White-rot fungi produce four major groups of enzymes for the degradation of lignin: lignin peroxidase (known as ligninase in early publications; LiP; EC 1.11.1.14), manganese-dependent peroxidase (manganese peroxidase, MnP; EC 1.11.1.13), versatile peroxidase (VP; EC 1.11.1.16), and laccase (EC 1.10.3.2). The process is further enhanced by the cooperative action of several accessory enzymes, which may include glyoxal oxidase (EC 1.2.3.5), aryl alcohol oxidase (veratryl alcohol oxidase; EC 1.1.3.7), pyranose 2-oxidase (glucose 1-oxidase; EC 1.1.3.4), cellobiose/quinone oxidoreductase (EC 1.1.5.1), and cellobiose dehydrogenase (EC 1.1.99.18). For reviews, see [23, 30–35].

Heme peroxidases form a superfamily of enzymes responsible for numerous biosynthetic and degradative functions. Based on their sequences and catalytic properties, the extracellular fungal LiP, MnP, and VP belong to class II peroxidases within the superfamily of heme peroxidases, which includes class I prokaryotic lineage peroxidases and class III classical secretory plant peroxidases [36]. The enzymes oxidize substrates in multi-step electron transfers with the formation of intermediate radical cation, similar to that observed in the well-known horseradish peroxidase.

Lignin Peroxidase

Lignin peroxidases [EC 1.11.1.14, 1,2-bis(3,4-dimethoxyphenyl)propane-1,3-diol:hydrogen-peroxide oxidoreductase] catalyze the H_2O_2-dependent oxidative depolymerization of lignin [37, 38]. The overall reaction is represented by 1,2-bis(3,4-dimethoxyphenyl) propane-1,3-diol + H_2O_2 ⇌ 3,4-dimethoxybenzaldehyde+1-(3,4-dimethoxyphenyl)ethane-1,2-diol + H_2O. LiP is relatively nonspecific to its substrates and has been known to oxidize phenolic aromatic substrates and also a variety of non-phenolic lignin model compounds as well as a range of organic compounds with a redox potential up to 1.4 V (versus normal hydrogen electrode) in the presence of H_2O_2 [39]. The enzyme activity of LiP is conveniently measured by the increase in absorbance at 310 nm in the oxidation of veratryl

alcohol (VA; 3,4-dimethyoxybenzyl alcohol), the favored LiP substrate, to veratraldehyde (VAD) by the increase in absorbance at 310 nm.

Molecular Structure

LiP was first discovered in *Phanerochaete chrysosporium*, and various isoforms are known to exist with this microorganism and also a number of other white-rot fungi. The LiP isozymes are glycoproteins of 38–46 kDa, with p*I* values of 3.2–4.0. LiP has a distinctive property of an unusually low pH optimum near pH 3. The enzyme contains 1 mol of iron protoporphyrin IX per mole of protein. The crystal structure of *P. chrysosporium* LiP has been described in details [40–43]. The enzyme is globular with a dimension of 50×40×40 Å comprised of a proximal (C-terminal) and distal (N-terminal) domain (Fig. 5). The heme is embedded in a crevice between the two domains, but is accessible from the solvent via two small channels. The enzyme molecule contains eight major and eight minor α-helices and a limited β structure in the proximal domain. An extended C-terminal segment of about 50 amino acids traverse over the surface with little contact to the core of the protein. The LiP has eight Cys residues, all forming disulfide bridges. There are two calcium-binding sites, one in each domain, with possible function of maintaining the topology of the active site. The enzyme is *N*-glycosylated at Asn257, and *O*-glycosylated at Ser334 and Thr320, all clustered at the upper portion of the proximal domain. The carbohydrate chains may play a role in the protection of the C-terminal peptide from proteolysis. The heme iron is predominantly high spin, pentacoordinated with His176–$N_{\varepsilon 2}$ at the proximal side as the fifth ligand, and Wat339 H-bonded to the distal His46–$N_{\varepsilon 2}$ (Fig. 6). The heme–porphyrin is nonplanar, with the iron displaced 0.1 Å toward the distal

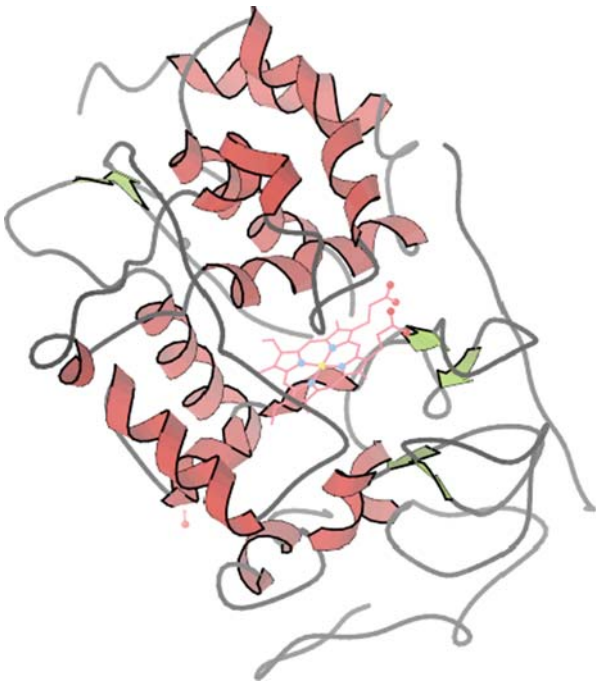

Fig. 5 Three-dimensional structure of *P. chrysosporium* lignin peroxidase ([41], PDB#1lga)

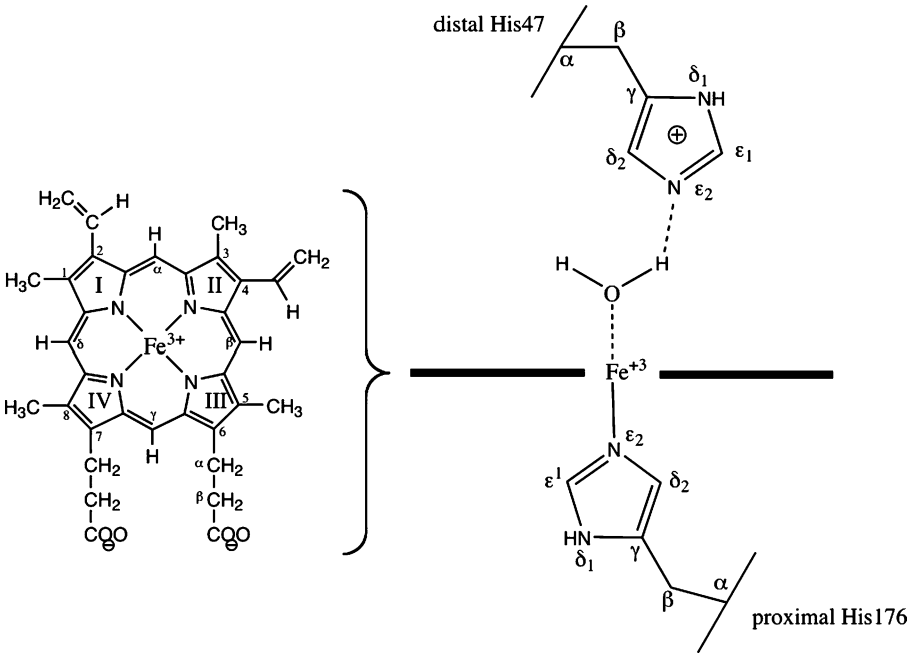

Fig. 6 The heme iron environment in lignin peroxidase

His residue. The peroxide-binding pocket is located on the distal side of the heme, with a channel extending to the exterior of the protein. The Arg43 functions in stabilizing negative charges developed in the cleavage of peroxides and in stabilizing the ferryl oxygen of compound I. The distal His47, hydrogen bonded with Asn82, acts as a proton acceptor for the bound peroxide substrate. In the proximal pocket, the His176 coordinates with the heme iron and also forms hydrogen bond with Asp235, which helps to stabilize the Fe(IV)–O intermediate in compound I. The Asp–His–Fe triad is conserved in peroxidases of the plant superfamily. A more recently detected structural feature is a posttranslational modification, a hydroxy group at the C_β of the surface residue Trp 171 [42, 44]. This Trp residue has been suggested an important role in the binding and oxidation of VA through long-range electron transfer, although the function of hydroxylation is not yet clearly established. Substitution of the Trp residue by a Ser or Phe leads to complete loss of activity [45]. Introduction of a Trp residue in wild-type MnP at the position corresponding to Trp171 in LiP results in the ability of the enzyme to oxidize VA and non-phenolic substrates [46, 47].

The Catalytic Cycle

LiP has a typical peroxidase catalytic cycle similar to horseradish peroxidase in many aspects [48]. The general mechanism of LiP catalyzed reaction consists of two steps [49]:

(1) A $2e^-$ oxidation of the native ferric enzyme [Fe(III)] to yield compound I intermediate that exists as a ferry iron porphyrin radical cation [Fe(IV)=$O^{\cdot+}$, LiP-I], with the peroxide substrate (H_2O_2) cleaved at the O–O bond (Fig. 7).

$$\mathrm{LiP[Fe(III)] + H_2O_2 \rightarrow LiP\text{-}I[Fe(IV) = O^{\cdot+}] + H_2O}$$

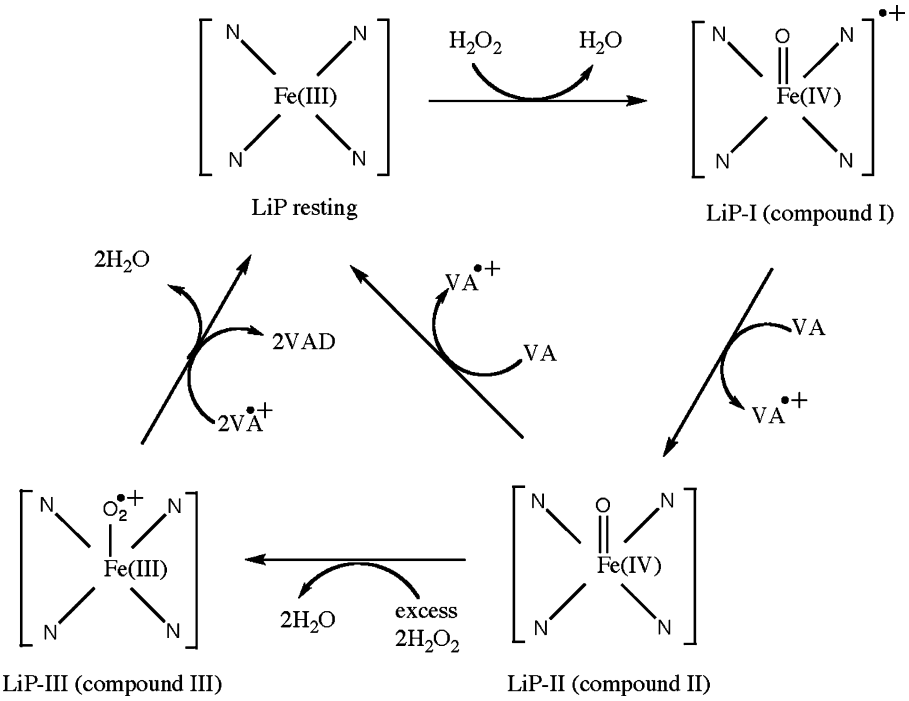

Fig. 7 Catalytic cycle of lignin peroxidase

(2) A two consecutive $1e^-$ reduction of LiP-I by electron donor substrates to the native enzyme. The first $1e^-$ reduction of LiP-I by a reducing substrate, such as VA, yields compound II [Fe(IV)=O, LiP-II] and a VA radical cation ($VA^{\cdot+}$). A second $1e^-$ reduction returns the enzyme to the ferric oxidation state, completing the catalytic cycle. LiP-I can also return to the native (resting) enzyme by a direct $2e^-$ reduction in some cases.

$$\text{LiP-I} + \text{AH} \rightarrow \text{LiP-II}[\text{Fe(IV)} = \text{O}] + \text{A}^{\cdot+}$$
$$\text{LiP-II} + \text{AH} \rightarrow \text{LiP} + \text{A}^{\cdot+}$$

Compound I

The native LiP reacts with H_2O_2 to form LiP-I with a second-order rate constant of 5.4×10^5 M^{-1} s^{-1}. The reaction is independent of pH from pH 2 to 7.5 [50, 51]. The reason for the lack of a pH effect on the reaction is not clear. H_2O_2 is the preferred substrate with a K_m value ~30 μM, although organic peroxides can also serve as substrates albeit with a lower rate constant. The heterolytic cleavage of the $O\alpha - O\beta$ bond of the peroxide substrate is facilitated by coordination of the heme Fe(III) and protonation by the distal His47. The departure of H_2O leaves a transient Fe(III)-O^+, followed by electron transfers from the Fe (III) and the porphyrin π electron system to form an oxyferryl complex Fe(IV)=O structure [52, 53]. LiP-I therefore has a heme structure of O=Fe(IV)-porphyrin π radical cation with S=3/2. It contains two oxidizing equivalent over the native LiP; the first located in the ferryl state of the iron as [Fe(IV)=O] structure (low spin, S=1) and the second in the

porphyrin π radical cation (S=1/2). Instead of the heme radical, the involvement of the surface Trp171 in a radical form via long-range electron transfer to the heme has also been suggested for H_2O_2-activated LiP [42, 54].

Compound II

The reaction of LiP-I with a reducing substrate to form LiP-II is pH dependent, with the rate decreased with increasing pH [51, 55]. With VA as the substrate, the rate is 2.5×10^6 M^{-1} s^{-1} at pH 3.1 and decreases dramatically with increasing pH. The subsequent reaction of LiP-II with a second molecule of reducing substrate to yield the native enzyme is also pH dependent and the rate is relatively slower (1.6×10^5 M^{-1} s^{-1}). It is clear that the pH dependence of the reduction of LiP-I and LiP-II rather than the formation of LiP-I dictates the unusual low pH optimum for the enzyme. In the first reduction step, the porphyrin π-cation radical first accepts an electron from the substrate, concomitant with a proton transfer to the distal His. LiP-II thus formed is one oxidation equivalent above the native LiP, with the porphyrin filled by the donor substrate. The heme therefore has a structure of an oxyferryl complex, Fe(IV)=O, as in LiP-I. In the second reduction step, the LiP-II oxyferryl forms hydrogen bonding with the protonated His, which then accepts an electron from a second substrate, to yield the native LiP, as known in other peroxidases [56]. Analysis of crystal structures suggests that the opening of the active site channel and the heme access channel are too small for reducing substrates, such as VA, for direct interaction with the ferryl oxygen [41, 43]. There is accumulation of evidence suggesting the substrate oxidized at the heme edge via a long-range electron transfer mechanism, probably mediated by the β-hydroxylated Trp171 residue on the enzyme surface [42, 45, 57]. Site-directed mutagenesis studies suggest the involvement of Trp171 and Phe267 residues in binding and oxidation of VA [45, 58, 59]. Molecular simulations of lignin peroxidase in solution suggest, however, the presence of deformation and enlargement of the access channel that can facilitate the movement of small natural substrates toward the active site [60].

Compound III

At pH 3.0, in the presence of excess H_2O_2 and the absence of a reducing substrate, LiP-II reacts with H_2O_2 to form a catalytic inactive form of the enzyme, known as compound III (LiP-III) [51, 61, 62] The heme of LiP-III exists as a ferric-superoxo complex [$Fe(III)O_2^{\cdot-}$]. LiP-III can be converted to the resting enzyme by spontaneous autoxidation or by oxidation with a VA radical cation through the displacement of superoxide from the active site [62, 63].

Phenolic and Non-phenolic Substrates

The association of ligninolytic enzymes with lignin breakdown arises because the enzyme can oxidize lignin-related aromatic compounds. Single-ring, aromatic substrates are frequently used, including phenolic compounds, such as guaiacol, vanillic acid, and syringic acid, and non-phenolic veratryl alcohol, and dimethylphenylenediamine. This type of substrates has been useful for characterization of catalytic cycles, particularly on the formation and reactions of the oxidized enzyme intermediates. Another group of substrates consists of lignin model dimers that are frequently used to investigate specific bond cleavages. These compounds are synthetic mimics of the common lignin substructures, such as diarylpropane and β-aryl ether dimer. The β-*O*-4 lignin model compounds are the most important type for elucidating lignin degradation, as arylglycerol β-aryl ether or β-*O*-4 bond is the most prevalent linkage type

in lignin, accounting for about 50% of the interunit connections in gymnosperm and 60% in angiosperm [6]. These model compounds can be synthesized either as phenolic or non-phenolic in nature. Phenolic subunits are present only about 10–20% in lignin [6]. However, demethylation and ether cleavage reactions in enzyme-catalyzed degradation can generate phenolic products, which can in turn be the substrate for further breakdown [64]. In general, cleavage of non-phenolic moieties, which comprises 80–90% in lignin, is the major indicator of enzymatic degradation.

Oxidation of Phenolic Substrates

Like other peroxidases, LiP is capable of oxidizing a wide variety of phenolic compounds including ring- and *N*-substituted anilines [65]. LiP catalyzes oxidation of phenolic compounds (guaiacol, vanillyl alcohol, catechol, syringic acid, acetosyringone, etc.) preferentially at a much faster rate compared to non-phenolic substrates [66]. In the reduction of LiP-I and LiP-II, phenolic substrates are converted to phenoxy radicals. In the presence of oxygen, the phenoxy radical may react to form ring-cleavage products, or they may otherwise also lead to coupling and polymerization [64, 67, 68]. Although repolymerization is generally observed in *in vitro* experiments, it is less likely with *in vivo* systems because of compartmentation of the enzyme, lignin and phenolic breakdown products [66]. Oxidation of guaiacol to tetraguaiacol by LiP exhibits classical Michaelis–Menton kinetics with a K_m of 160 μM and a k_{cat} of 7.7 s^{-1} at 28°C and pH 3.5 [69]. It has been reported that LiP-catalyzed oxidation of the lignin model dimer compound 1,2-di(3,4-methoxyphenyl)-1,3-propanediol results in $C_\alpha - C_\beta$ cleavage to yield veratraldehyde [70]. LiP-catalyzed oxidative reaction of phenolic compounds is typically associated with rapid decrease in enzyme activity [66]. The decrease is likely caused by the accumulation of the inactive LiP-III during catalysis. Phenoxy radicals, unlike the non-phenolic veratryl alcohol discussed below, are unable to revert LiP-III to the native enzyme, although both substrates show similar rate constants for the reaction of LiP-I [71]. The reactivity of phenolic compounds with LiP-I is much higher than that with LiP-II, and the rate constant decreases as the size of the substrate increases as demonstrated in the oxidation of oligomers of phenolic β-*O*-4 lignin model compounds [72].

Oxidation of Non-phenolic Substrates

Oxidative reaction of non-phenolic diarylpropane and β-*O*-4 lignin model compounds of lignin involves initial formation of radical cation via $1e^-$ oxidation, followed by side-chain cleavage, demethylation, intramolecular addition, and rearrangements (Figs. 8 and 9) [73–80]. Oxidation of the A ring giving rise to $C_\alpha - C_\beta$ cleavage is the major route [73, 81]. In the mechanism, only the formation of the radical cation is enzyme catalyzed, and subsequent reactions of the substrate are nonenzymatic. Decay of the radical cation depends on the nature of the substituents on the aromatic ring [82, 83]. Electron-donating groups, such as alkoxy groups, on the aromatic ring favor the formation and stabilization of the aryl radical cation [84].

Oxidation of Veratryl Alcohol

Veratryl alcohol is a metabolite produced at the same time as LiP by *P. chrysosporium* [85]. The addition of VA is known to cause an increase in LiP activity and the rate of lignin mineralization [86, 87]. It has been well established that VA ($E'_o = 1.36$) is oxidized by

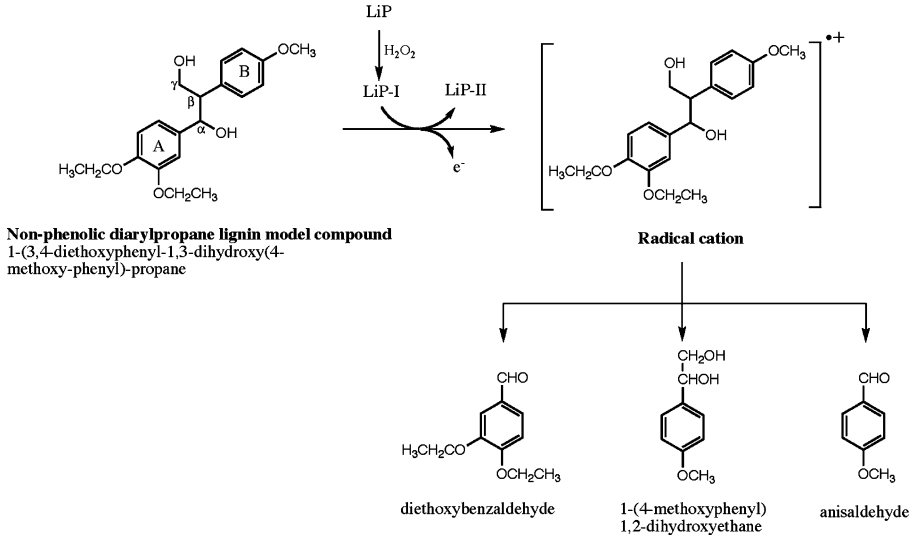

Fig. 8 LiP-catalyzed oxidation of non-phenolic diarylpropane lignin model dimer [73]

LiP-I and LiP-II, resulting in the formation of veratryl alcohol radical cation intermediate, $VA^{\cdot+}$ [88–90]. At pH 6.0, the second-order rate constant for LiP-catalyzed oxidation of VA is similar to that of β-*O*-4 dimer (6.7×10^3 and 6.5×10^3 M^{-1} s^{-1}, respectively) [81]. The radical cation formed in the first reduction by LiP-I exists as a complex with LiP-II, which is catalytically active on a second VA molecule to form an aldehyde [91]. The $VA^{\cdot+}$ generated in the reduction step decays by deprotonation at C_α, a typical reaction of alkyaromatic radical cations, to form veratraldehyde (Fig. 10) [92]. Under aerobic condition, however, additional oxidative pathways involving activated oxygen species occur leading to quinone formation and aromatic ring cleavage [93–95]. The mechanism is initiated by the attack of O_2 on the VA radical cation to yield an intermediate peroxy radical cation ($VAOO^{\cdot+}$), followed by reaction with nucleophilic solvent water.

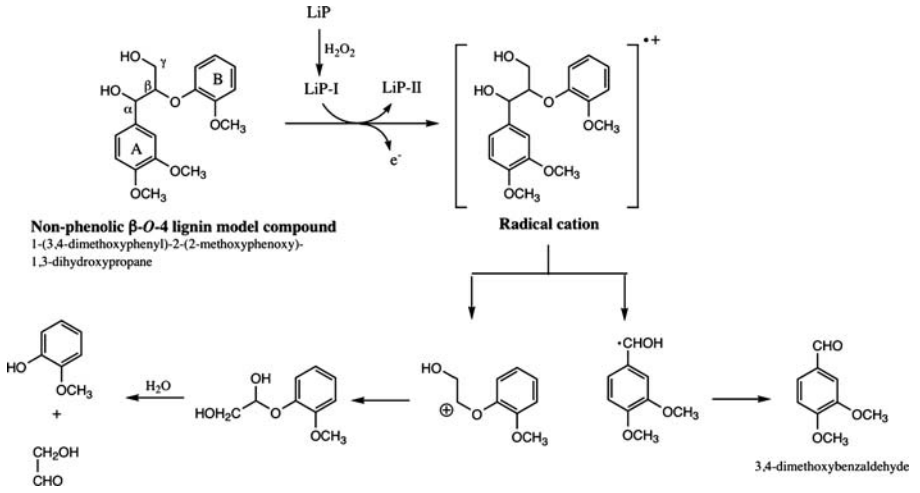

Fig. 9 LiP-catalyzed oxidation of non-phenolic β-*O*-4 lignin model compound [76, 81]

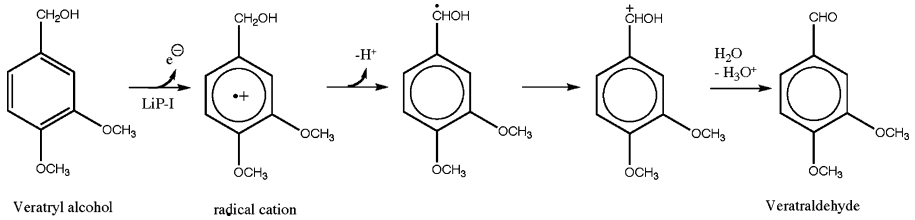

Fig. 10 Decay of veratryl alcohol radical cation by $C\alpha$ deprotonation [92])

The role of VA in lignin degradation has been the subject of several proposals. One suggestion considers $VA^{\cdot+}$ as a redox mediator in the oxidation of lignin [89]. $VA^{\cdot+}$ is capable of mediating oxidation of secondary substrates typically not oxidized by LiP [69, 89, 96–98]. The radical cation has also been implicated in the protection of LiP from inactivation because of the formation of LiP-III by prolonged incubation with or in excess of H_2O_2. In this case, VA converts LiP-III to the native enzyme via the formation of $VA^{\cdot+}$, potentially making more enzymes active for the oxidation of lignin [39]. The mediation model provides a mechanism by which LiP oxidizes the lignin substrate indirectly, with $VA^{\cdot+}$ diffusing from the enzyme to act as direct oxidant on lignin. Measurement of the lifetime of $VA^{\cdot+}$ suggests that it is able to act as a diffusible oxidant [92, 99, 100]. Other studies, however, suggests that $VA^{\cdot+}$ is unstable and hence unlikely to effect long-range oxidation in LiP-catalyzed reactions [101].

The High Redox Potential of Lignin Peroxidase

Although mechanistically very similar to HRP and other peroxidases, LiP is unique in its ability to oxidize substrates of high redox potentials. This is in addition to the low pH optimum near pH 3.0 and sensitivity to excess H_2O_2 for activity described above. LiP-I stores a high redox potential (E'_o ~1.2 V at pH 3.0) that enables it to catalyze the oxidation of non-phenolic aromatic substrates not normally associated with other peroxidases [102]. The redox potential decreases linearly as the pH increases, but is not affected by the substrate. The high redox potential for the Fe(III)/Fe(II) couple are consistent with the heme active sites being more electron deficient than other peroxidases. In contrast, the Mn(III)-malonate/oxalate complex in MnP has a redox potential near 0.80 V at pH 4.5 [103]. The redox potential for laccase has been reported as 0.79 V (basidiomycetes *T. versicolor* T1/T3, pH 5.5), 0.47 V (ascomycete *Myceliophthora thermophila*, pH 6.0), and 0.39 V (plant *Rhus verniciera* T1/T3, pH 7.5) [104, 105]. Horseradish peroxidase has a redox potential of 0.95 V at pH 6.3, whereas cytochrome c peroxidase has a value of 0.19 V at pH 7 [106, 107]. A comparison of LiP, MnP, and laccase in the oxidation of a homologous series of 12 methoxybenzenes (ranged from 0.81 to 1.76 V at pH 3.0) shows the reaction correlated to the redox potentials of the enzyme and the compound substrate [102, 108]. Lignin peroxidase with the highest redox potential oxidizes ten methoxybenzene congeners ($E'_o = 0.81$ to 1.49 V), whereas MnP and HRP with lower redox potentials oxidize only four congeners ($E'_o = 0.81$ to 1.12 V), and laccase only oxidizes 1,2,4,5-tetramethoxybenzene, the lowest redox potential congener ($E'_o = 0.81$ V). Thus, LiP is a stronger oxidant than MnP, which in turn is stronger than laccase, and LiP does not require the participation of mediators in the oxidation of non-phenolic substrates.

Manganese Peroxidase

Manganese peroxidase [EC 1.11.1.13, Mn(II):hydrogen-peroxide oxidoreductase, MnP] catalyzes the Mn-dependent reaction $2Mn(II)+2H^{+}+H_2O_2=2Mn(III)+2H_2O$. The first extracellular MnP was purified from *P. chrysosporium*, with its expression and production shown to be regulated by the presence of Mn(II) in the culture medium [109]. Mn(II) controls the *mnp* gene transcription that is growth and concentration dependent [110, 111]. MnP is also regulated at the level of gene transcription by heat shock and H_2O_2 [112]. In addition to the stimulatory effect of Mn(II), organic acids, such as glycolate, malonate, glucuronate, 2-hydroxybutyrate, added to the medium enhances the production of MnP by the white-rot fungus *Bjerkandera* sp. strain BOS55 [113]. *Bjerkandera* species also produces versatile peroxidase that possesses both Mn-mediated and Mn-independent activity as described in the later section. Mn(II) also downregulates LiP titer in white-rot fungus, because of its suppression of the production of veratryl alcohol, which has been postulated to function in protecting LiP from inactivation by high levels of H_2O_2 [114].

Molecular Structure

The *P. chrysosporium* enzyme is an acidic glycoprotein with a p*I* near 4.5 and a Mr of 46,000. MnP is produced as a series of isozymes often coded and differentially regulated by different genes [115]. MnP contains one molecule of heme as iron protoporhyrin IX and shows a maximal activity at Mn(II) concentrations above 100 μM [116]. The heme iron in the native protein is in the high-spin, pentacoordinate, ferric state with a His residue coordinated as the fifth ligand [117]. The overall structure of *P. chrysosporium* MnP is similar to LiP, consisting of two domains with the heme sandwiched in-between (Fig. 11) [118]. The protein molecule contains ten major helices and one minor helix as found in LiP. MnP has five rather than four disulfide bonds, with the additional bond, Cys341–Cys348, located near the C terminus of the polypeptide chain. This additional disulfide bond helps to form the Mn(II)-binding site and is responsible for pushing the C terminus segment away from the main body of the protein. The distal His46 is hydrogen bonded to Asn80 to ensure that $N_{\varepsilon 2}$ is available to accept a proton from the peroxide in acid-base catalysis. The H bond formed between the proximal His173 and the side chain of Asp242 increases the anionic character of the ligand and helps stabilizing the oxyferry iron in MnP-I. The Mn(II) is located in a cation-binding site at the surface of the protein and coordinates to the carboxylate oxygens of Glu35, Glu39, and Asp179, the heme propionate oxygen, and two water oxygens. The site has considerable flexibility to accommodate the binding of a wide variety of metal ions [119, 120]. Two heptacoordinate structural calcium ions, one tightly bound on the proximal side and the other bound on the distal side of the heme, are important for thermal stabilization of the active site of the enzyme [119].

The Catalytic Cycle

Mn-dependent peroxidases are unique in utilizing Mn(II) as the reducing substrate [116, 121, 122]. MnP oxidizes Mn(II) to Mn(III), which in turn oxidizes a variety of monomeric phenols including dyes as well as phenolic lignin model compounds. The catalytic cycle

Fig. 11 Three-dimensional structure of *P. chrysosporium* manganese peroxidase ([120], PDB 1yyd)

thus entails the oxidation of Mn(II) by compound I (MnP-I) and compound II (MnP-II) to yield Mn(III).

$$\mathrm{MnP} + \mathrm{H_2O_2} \rightarrow \mathrm{MnP\text{-}I} + \mathrm{H_2O}$$
$$\mathrm{MnP\text{-}I} + \mathrm{Mn^{2+}} \rightarrow \mathrm{MnP\text{-}II} + \mathrm{Mn^{3+}}$$
$$\mathrm{MnP\text{-}II} + \mathrm{Mn^{2+}} \rightarrow \mathrm{MnP} + \mathrm{Mn^{3+}} + \mathrm{H_2O}$$

Mn(III) in turn mediates the oxidation of organic substrates.

$$\mathrm{Mn^{3+}} + \mathrm{RH} \rightarrow \mathrm{Mn^{2+}} + \mathrm{R^{\cdot}} + \mathrm{H^{+}}$$

The characteristics of the cycle are very similar to that of LiP. Addition of 1 equivalent of H_2O_2 to the native enzyme yields MnP-I, which is a Fe(IV)-oxo-porphyrin radical cation [Fe(IV)=O$^{\cdot+}$]. The peroxide bond of H_2O_2 is cleaved subsequent to a $2e^-$ transfer from the enzyme heme-porphyrin. The formation of MnP-I is pH independent, with a second-order rate constant of 2.0×10^6 M^{-1} s^{-1} [123]. Addition of 1 equivalent to Mn(II) rapidly reduces compound I to compound II. The conversion of MnP-I to MnP-II can also be achieved by the addition of other electron donors, such as ferrocyanide and a variety of phenolic compounds [124]. In the reduction of compound II to generate the native enzyme, however, Mn(II) is an obligatory redox coupler for the enzyme to complete its catalytic cycle.

Mn(III) Chelators

The Mn(III) formed is dissociated from the enzyme and stabilized by forming complexes with α-hydroxy acids at a high redox potential of 0.8–0.9 V. Oxalate and malonate are optimal

chelators that are secreted by the fungus in significant amounts [125, 126]. It has also been shown that MnP reacts with oxalate–Mn(II) instead of free Mn(II) as the true substrate with the chelator involved in the redox reaction of the metal [127]. Other physiological functions have been associated with these chelators, including the enhancement of enzyme activity by their ability to facilitate the dissociation of Mn(III) from the enzyme. Oxalate has been proposed to function as an extracellular buffering agent, allowing the fungus to control the pH of its environment [128]. It may also act as calcium sequester to increase the pore size of the plant cell wall and to facilitate the penetration of enzyme molecules. Oxidation of oxalic acid by Mn(III) produces a formate radical ($HCO_2^{\cdot}$) that reacts with dioxygen to form superoxide ($O_2^{\cdot-}$) and, subsequently, H_2O_2 [129, 130]. This process has also been implicated in contributing to the ability of the fungus to degrade lignin.

Oxidation of Phenolic Substrates

The Mn(III) chelator complex acts as a diffusible oxidant of phenolic substrates involving $1e^-$ oxidation of the substrate to produce a phenoxy radical intermediate, which undergoes rearrangements, bond cleavages, and nonenzymatic degradation to yield various breakdown products (Fig. 12) [122, 131, 132]. MnP-generated Mn(III) can catalyze the oxidation of phenolic substrates, including simple phenols, amines, dyes, as well as phenolic lignin substructure and dimers. Mn(III) chelator is a mild oxidant under physiological conditions limited to the oxidation of phenolic lignin structures and, by itself, is not capable of oxidizing non-phenolic compounds [38].

Oxidation of Non-phenolic Substrates

For non-phenolic substrates, the oxidation by Mn(III) involves the formation of reactive radicals in the presence of a second mediator [133]. This is in contrast to that of LiP-catalyzed reaction, which involves electron abstraction from the aromatic ring forming a radical cation. Mn(III) in the presence of thiols, such as glutathione, mediates the oxidation of substituted benzyl alcohols and diarylpropane structures to their respective aldehydes [133, 134]. In these reactions, Mn(III) oxidizes thiols to thiyl radicals, which subsequently

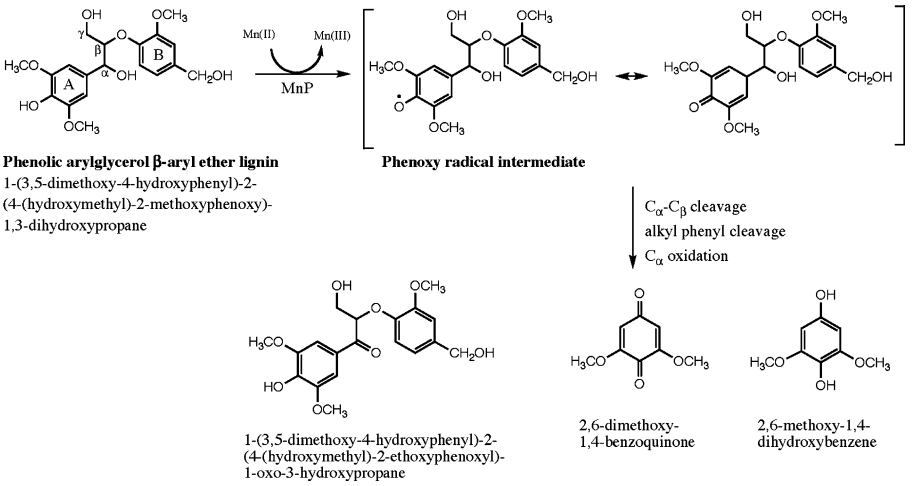

Fig. 12 MnP-catalyzed oxidation of phenolic aryglycerol β-aryl ether lignin model compound [132]

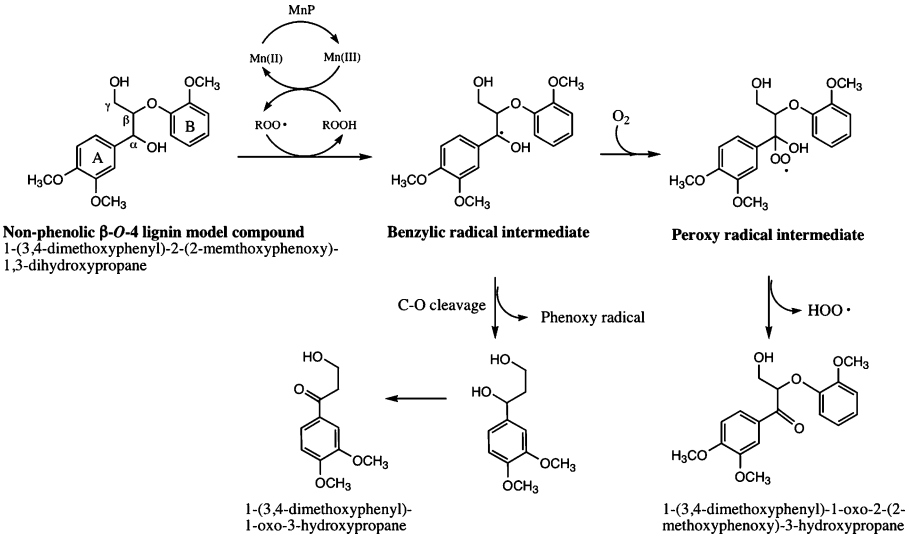

Fig. 13 MnP-catalyzed oxidation of non-phenolic β-*O*-4 lignin model compound [135, 138]

abstract hydrogen from the substrate to form a benzylic radical. The latter undergoes nonenzymatic reactions to yield the final products.

The enzyme generated Mn(III) also couples with peroxidation of lipids to catalyze $C_\alpha - C_\beta$ cleavage and β-aryl ether cleavage of non-phenolic diarylpropane and β-*O*-4 lignin structures, respectively (Fig. 13) [133, 135–138]. The mechanism involves hydrogen abstraction from the benzylic carbon (C_α) via lipid peroxy radicals, followed by O_2 addition to form a peroxy radical, and subsequent oxidative cleavage and nonenzymatic degradation.

In the absence of exogenous H_2O_2, the enzyme oxidizes nicotinamide adenine dinucleotide phosphate (reduced form), glutathione, dithiothreitol, and dihydroxymaleic acid, generating H_2O_2. This oxidase activity of MnP has implications in fungal lignin degradation, because the H_2O_2 produced may become available for the enzyme to start the peroxidase cycle [122]. The H_2O_2 could also be utilized by lignin peroxidase, which is H_2O_2 dependent for catalytic activity.

Compound III

Similar to LiP and other peroxidases, MnP-II reacts with additional H_2O_2 to form a Fe(III)-superoxo complex as compound III (MnP-III), which can be further oxidized by H_2O_2 resulting in heme bleaching and irreversible inactivation of the enzyme. The rate of MnP inactivation is one order of magnitude lower than that of LiP [139]. The reactivation of MnP-III is mediated by Mn(III), which interacts either by oxidizing the iron-coordinated superoxide or reacting with H_2O_2 in a catalase-type activity [140]. This mechanism is in contrast to LiP where LiP-III is oxidatively converted back to the native LiP by the radical cation of aromatic substrates.

Laccase

Laccases (EC 1.10.3.2, benzenediol:oxygen oxidoreductase) belong to a family of multi-copper enzymes, which include ascorbic oxidase and ceruloplasmin. The enzyme catalyzes

the overall reaction: 4 benzenediol+O_2↔4 benzosemiquinone+2H_2O. Laccases represent one of the oldest enzymes ever described [141]. The enzyme seems ubiquitous in all white-rot fungi investigated, and its presence is less frequent in plants. The better-characterized enzymes are from the fungus *T. versicolor* and the Japanese lacquer tree *R. vernicifera* (hence the name laccase). Laccase activities are also found in some bacterial species [142–144]. The plant enzyme is involved in wound response and participates together with peroxidases in the biosynthesis of lignin [145–147]. Fungal laccase plays a role in pigment formation in spores, detoxification of phenol compounds produced during lignin degradation and acts synergistically with peroxidases and other enzymes in the breakdown of lignin [148–150].

Molecular Structure

Fungal laccases occur often as isozymes with monomeric or dimeric protein structures. Both intracellular and extracellular isozymes may be produced from a single organism. The monomeric proteins have a molecular mass ranging from 50 to110 kDa [151]. The fungus *T. versicolor* produces five isozymes, depending on the degree of glycosylation [152]. Laccases are approximately 10–45% glycosylated with the fungal enzyme less substituted than the plant enzyme. The three-dimensional structures of the following fungal laccases have been reported: *Coprinus cinereus* in the type-2 Cu-depleted form, *T. versicolor*, *Pycnoporus cinnabarinus*, *Melanocarpus albomyces*, and *Rigidoporus lignosus* with full complement of copper ions [153–157]. The CotA laccase from *Bacillus subtilis* has been structurally characterized [158]. All fungal laccases show a similar architecture consisting of three sequentially arranged domains of a β-barrel type structure, related to the small blue copper proteins, such as azurin and plastocyanin (Fig. 14).

The active site is well conserved—It contains four copper sites, type 1 (T1, one Cu atom), type 2 (T2, one Cu atom), and type 3 (T3, two Cu atoms) per molecule (Fig. 15). In the resting enzymes, all four coppers are in the 2+ oxidation state [159, 160]. T1 is located in domain 3 with the copper lying in a shallow depression on the surface of the enzyme. T2 and T3 form a trinuclear copper cluster (T2/T2) at the interface between domains 1 and 3 with each domain providing ligand residues for the coordination of the copper atoms.

The T1 copper has unique features of an electron paramagnetic resonance (EPR) signal (i.e. paramagnetic) and an intense absorption band ($\Delta\varepsilon$=~5,000) at 610 nm (hence known as blue copper site). The T1 copper is coordinated with two His-$N_{\delta 1}$ and a Cys thiolate sulfur as conserved equatorial ligands. The axial position has a Leu or Phe present that does not participate in the coordination. The copper-thioether bond as well as the non-coordination residues in the axial position strongly influences the redox potential of the enzyme [161]. The T1 site is the primary electron acceptor site where the enzyme catalyzes four $1e^-$ oxidations of a reducing substrate. The electrons extracted from the reducing substrate are transferred to the T2/T3 trinuclear center where dioxygen reduction to water occurs.

The T2/T3 trinuclear site is where the reduction of molecular oxygen takes place by accepting electrons transferred from the T1 site. The T2 copper is coordinated to two His-$N_{\varepsilon 2}$ and one oxygen atom as OH^-, forming a trigonal coplanar configuration. Each of the T3 coppers coordinates to three His residues and a bridging oxygen atom, having a distorted tetrahedral geometry. The T2 copper is paramagnetic and exhibits no intense absorption peaks. The T2 site has affinity to azide, fluoride, and cyanide as inhibitors. T3 copper pair (Cu3a and Cu3b) has an absorbance at 330 nm ($\Delta\varepsilon$=2,800 M^{-1} cm^{-1}) and is EPR silent (anti-ferromagnetic) because of the bridging of the copper pair.

Fig. 14 3D structure of *T. versicolor* laccase ([154], PDB#1gyc)

Laccases from different sources exhibit a wide range of redox potentials. The T1 site has a high redox potential reaching 780 to 800 mV for the *T. versicolor* and *Neurospora crassa* enzymes, whereas the plant *R. vernicifera* enzyme has a value of 420 mV [154, 159, 162]. The redox potentials of T2 and T3 sites for the *R. vernicifera* laccase are, respectively, 390 and 460 mV at pH 7.5 [162]. The *T. versicolor* laccase T1 and T3 sites have been reported to be 785 and 782 mV, respectively [104]. In general, the T1 sites in fungal laccases are much higher than those of plant laccases and other blue copper oxidases, although significant differences in potentials also exist among fungal laccases [163]).

Laccases exhibit low substrate specificity and can oxidize a range of compounds, such as diphenols, aryl diamines, and aminophenols. The K_m values are generally in the range of 1–10 mM, and the change in $\log(k_{cat}/K_m)$ increases proportionally to the redox potential difference between the T1 site acceptor and the substrate donor [164].

Mechanism of Catalysis

Laccases catalyze four $1e^-$ oxidation of a reducing substrate with concomitant two $2e^-$ reduction of dioxygen to water. The stochiometry is four molecules of reducing substrate for each molecular oxygen, involving a total transfer of four electrons [$4RH+O_2 \rightarrow 4R+2H_2O$].

The first step of catalysis is reduction of the reducing substrate by the copper (Cu^{2+} to Cu^{+}) at the T1 site, which is the primary electron acceptor [165–167]. The electrons extracted from the reducing substrate are transferred to the T2/T3 trinuclear site, resulting in the conversion of the resting form (fully oxidized) of the enzyme to a fully reduced state. A

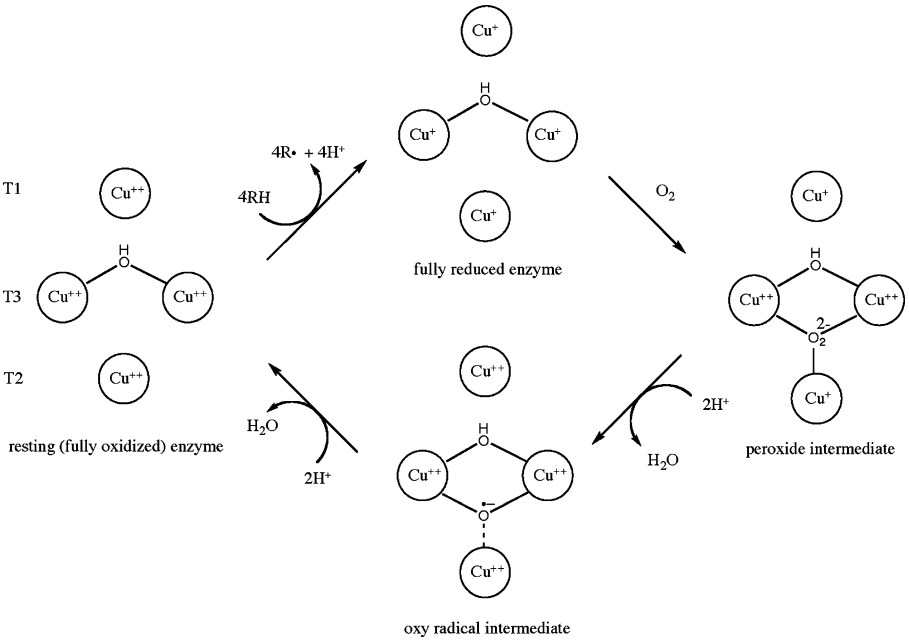

Fig. 15 Catalytic cycle of laccase

successive $4e^-$ oxidation (from four substrate molecules) is required to fully reduce the enzyme (Fig. 15). The e^- transfer from the substrate to the T1 copper is not a rate-limiting step in the overall reaction, but the intramolecular electron transfer from T1 to the trinuclear copper site is rate limiting in the catalytic cycle.

Reduction of dioxygen takes place in two steps via the formation of bound oxygen intermediates. The dioxygen molecule first binds to the T2/T3 site, and two electrons are rapidly transferred from the T3 coppers, resulting in the formation of a peroxide intermediate. The peroxide bridges between the oxidized T3 and the reduced T2 copper sites, although the configuration of the oxygen has not been fully established. The diffusion of dioxygen to the trinuclear site is rate limiting, followed by a rapid $1e^-$ transfer from T1. The peroxide intermediate decays to an oxy radical and undergoes a $2e^-$ reductive cleavage of the O–O bond with the release of a water molecule [168, 169]. The slow decay of the intermediate is facilitated by the final electron transfer from the T2 copper, and is accelerated with decreasing pH, with protonation from a carboxylic acid residue near the active site [170]. In the last step, all four copper centers are oxidized, and O^{2-} is released as a second water molecule. The reoxidation of the T2 copper correlates with the decay of the intermediate in which the first water is released and the second water molecule remains bound and slowly exchanged with the bulk solution.

Oxidation of Phenolic Substrates

Laccases catalyze subtraction of one electron from phenolic hydroxyl groups of phenolic lignin model compounds, such as vanillyl glycol, 4,6-di(*t*-butyl)guaiacol, and syringaldehyde, to form phenoxy radicals, which generally undergo polymerization via radical coupling. The reaction is also accompanied by demethylation, formation of quinone, resulting in ring cleavage [171–173]. The degradation of phenolic β-1 lignin substructure

models occurs via the formation of phenoxy radicals that leads to $C_\alpha - C_\beta$ cleavage, C_α oxidation, alkyl-aryl cleavage, and aromatic ring cleavage (Fig. 16) [172, 174]. Laccase-catalyzed oxidation of phenols, anilines, and benzenethiols correlates with the redox potential difference between laccase's T1 copper site and the substrate [164]. The presence of electron-withdrawing *o*- and *p*-substituents reduces the electron density at the phenoxy group and, hence, more difficult to be oxidized (less susceptible to electron transfer to the T1 copper site). Bulky substituents, which impose steric interference with substrate binding, cause a decrease in reactivity.

Oxidation of Non-phenolic Substrates

LiP and MnP/mediator systems are able to oxidized non-phenolic models; however, some white-rot fungi, such as *Pycnoporus cinnabarinus*, lack LiP or MnP, but produce laccase as the predominant enzyme, and still degrade lignin very efficiently [150]. Accordingly, degradation of non-phenolic lignins must occur in these fungi. Laccase has been found to oxidize non-phenolic model compounds and β-1 lignin dimers in the presence of a mediator, indicating that the enzyme plays a significant role in depolymerization of lignin and pulp delignification [175].

The more studied mediators are 2,2′-azinobis-(3-ethylbenzthiazoline-6-sulfonate) (ABTS), 1-hydroxybenzotriazole (HBT), and 3-hyroxyanthranilic acid (HAA) [170, 176]. The latter is a natural mediator found to be produced in the culture of *Pycnoporous cinnabarinus* [177]. The oxidation is different for ABTS and HBT involving a di-cation and a benzotriazolyl-1-oxide radical, respectively [176]. Oxygen uptake by laccase is faster with ABTS than HBT, but the oxidation of non-phenolic substrate is comparable for both mediators. ABTS-mediated oxidation of non-phenolic substrate proceeds via an electron transfer mechanism [178, 179]. ABTS is first oxidized to the radical cation ($ABTS^{\cdot+}$) and

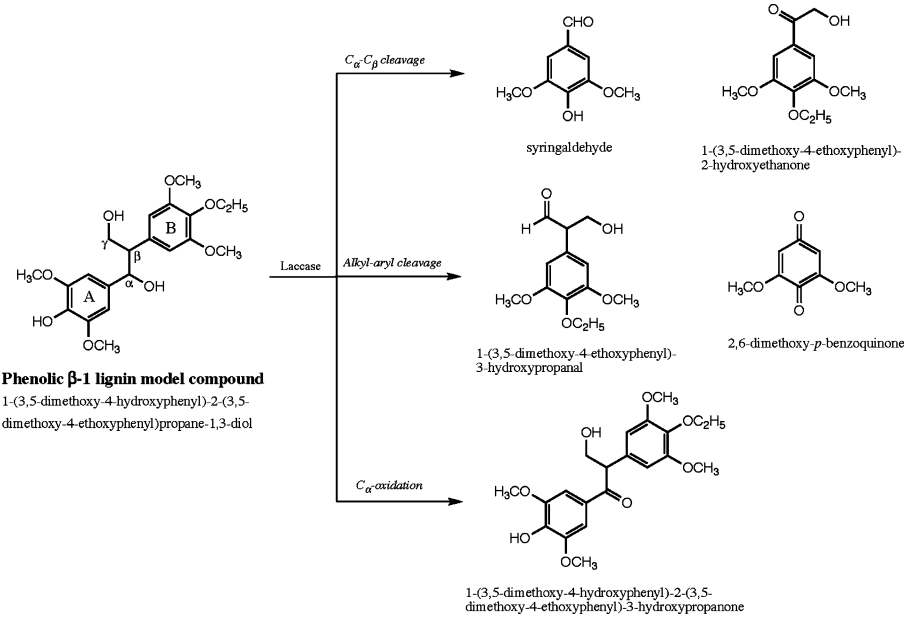

Fig. 16 Laccase-catalyzed oxidation of phenolic β-1 lignin model compound [172, 174]

then to the di-cation ($ABTS^{2+}$) with redox potentials of 472 mV ($ABTS/ABTS^{\cdot+}$) and 885 mV ($ABTS^{\cdot+}/ABTS^{2+}$), respectively [180]. The di-cation is the active intermediate responsible for the oxidation of the non-phenolic substrate. HBT-mediated oxidation of non-phenolic substrate involves initial oxidation of HBT to HBT^{+} by laccase, followed by immediate deprotonation to form the *N*-oxy radical. The latter abstracts the benzylic H-atom from the substrate, converting it to a radical. The oxidation of veratryl alcohol by laccase-ABTS (ET mechanism) and by laccase-HBT (radical H abstraction mechanism) is presented in Fig. 17 [178]. $HBT/HBT^{\cdot+}$, with an $E_o^{'}$ value of 1.08 V, has a mediator efficiency with laccase that is higher than that of the ABTS [178, 179]. The use of laccase/HBT for bleaching of paper pulps and for the removal of lipophilic extractives has been described [181–183]. Recently, two lignin-derived phenols, syringaldehyde and acetosyringone, have been shown to act as effective laccase mediators for the removal of lipophilic compounds from paper pulp [184].

The degradation of non-phenolic β-*O*-4 model compounds, which represent the major substructure in lignin, has been studied using laccase-mediator systems. Four types of reactions, β-ether cleavage, $C_\alpha - C_\beta$ cleavage, and C_α-oxidation and aromatic ring cleavage, are catalyzed by laccase–BHT coupled system [170, 172, 174]. In the oxidation of

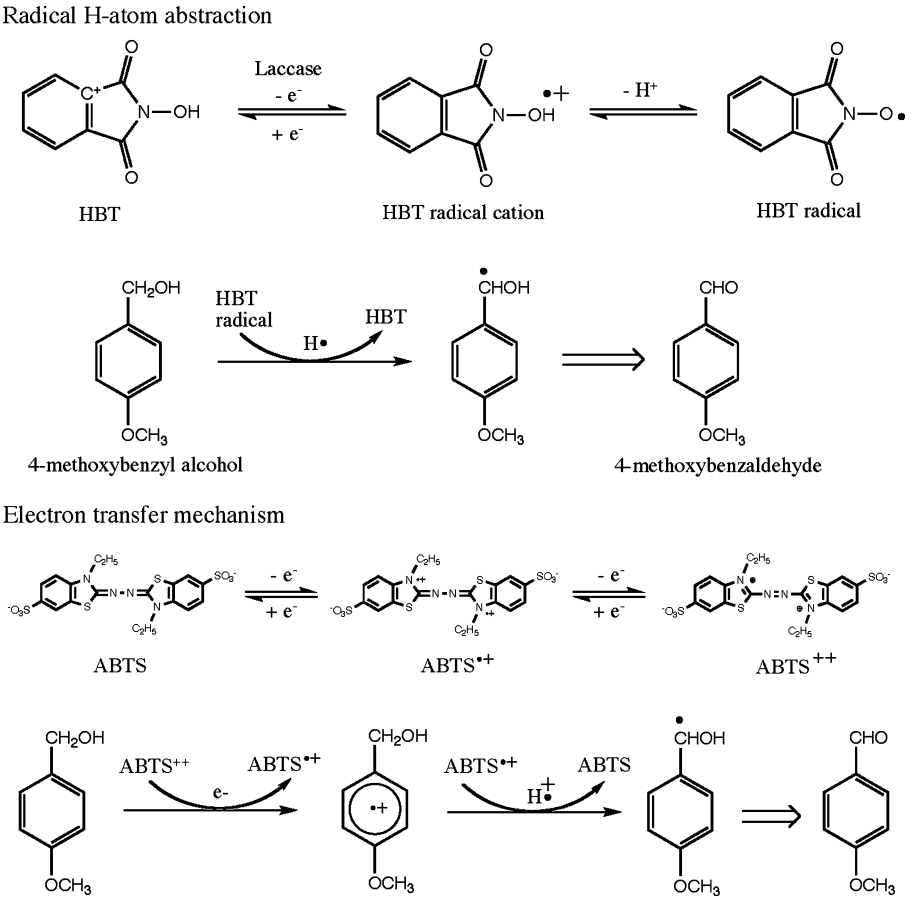

Fig. 17 Radical H-atom abstraction and electron transfer mechanisms [178]

a non-phenolic β-*O*-4 lignin model dimer, 1-(4-ethoxy-3-mthoxyphenyl)-1,3-dihydroxy-2-(2,6-dimethoxyphenoxy)propane, the coupled enzyme/HBT system catalyzes $1e^-$ oxidation of the substrate to form β-aryl radical cation or benzylic (C_α) radical intermediates [185, 186] (Fig. 18). Electron density of the aromatic ring affects the $1e^-$ oxidation by the laccase/1-HBT couple. Substrates containing electron-donating groups favor aromatic ring cleavage products. The β-aryl radical cation is converted to the product via an aromatic ring cleavage, and the benzylic radical is cleaved at the $C_\alpha - C_\beta$ bond similar to a Baeyer–Villiger reaction. The β-ether cleavage of the β-*O*-4 lignin substructure is caused by reaction with the C_α-peroxy radical intermediate produced from the benzylic radical [186]. The rate of oxidation depends on the k_{cat} of the laccase for the mediator and the stability of the enzyme to inactivation by the free radical of the mediator [187]. Because the non-phenolic lignin model dimer is chemically oxidized by the HBT radical, it may infer that oxidation of the C_α in the substrate occurs more easily than that of the π electron in the aromatic ring [188]. The work on oxidation of veratryl alcohol may also infer that laccase/ABTS favors the formation of aryl radical intermediate, while laccase/HBP proceeds with the benzylic radical formation.

Versatile Peroxidase

It has been reported that some manganese peroxidases isolated from fungi, *B. adusta*, *Bjerkandera* sp. strain BOS55, *Bjerkandera* sp. (B33/3), *B. fumosa*, *P. eryngii*, *P. ostreatus* and *P. pulmonaius*, exhibit activities on aromatic substrates similar to that of LiP [189–197]. This group of enzymes, known as versatile peroxidases, is not only specific for Mn (II) as in MnP, but also oxidizes phenolic and non-phenolic substrates that are typical for

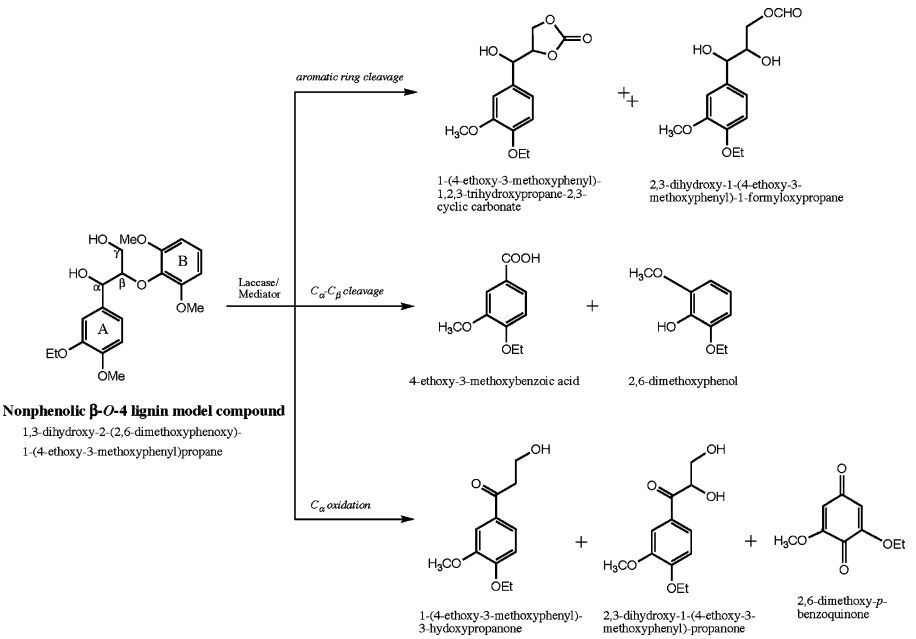

Fig. 18 Laccase-catalyzed oxidation of non-phenolic β-*O*-4 lignin model compound [185]

LiP, including veratryl alcohol, methoxybenzenes, and lignin model compounds, in the absence of manganese.

Molecular Structure

Molecular characterization of VP enzymes reveals structures closer to the LiP than to the MnP isozymes of *P. chrysosporium*, [190, 192, 198, 199]. A Mn(II) binding site containing acidic Glu/Glu/Asp residues typical of MnP enzymes is found near the heme internal propionate. In addition, residues involved in LiP interaction with VA and other aromatic substrates are also found in the protein structure. The molecular model of the *P. eryngii* versatile peroxidase shows 12 helices, 4 disulfide bonds, a heme pocket containing characteristic distal His47 and proximal His169, 2 structural Ca^{2+} sites, and a Mn(II) binding site (Fig. 19). In addition, a propionate of heme ring III enables Mn(II) fixation and electron transfer to compound I porphyrin ring or compound II Fe(IV)=O [198, 200]. The Mn(II) is coordinated by the heme propionate D and by the carboxylates of Glu36, Glu40, and Asp175, as evidenced by site-directed mutagenesis studies [199]. A surface solvent-accessible Trp164 has been identified in the oxidation of high redox potential aromatic substrates, such as veratryl alcohol via long-range electron transfer pathway [201]. Molecular modeling of *Bjerkandera* sp. B33/3 VP has shown that a similar Trp residue 170 is connected to the proximal His175 through a long-range electron transfer path involving several amino acids, with a distance of 10Å. An analogous Trp171 residue at the protein surface of the *P. chrysosporium* LiP has also been implicated in the long-range electron transfer pathway [54, 202].

Fig. 19 Three-dimensional structure of *P. eryngii* versatile peroxidase [200], PDB#2boq)

The Catalytic Cycle

The catalytic cycle for VP is similar to that of LiP and other heme peroxidases, in that the enzyme catalyzes the electron transfer from an oxidizable substrate, involving the formation and reduction of compound I and compound II intermediates. Compound I is a two-oxdizing equivalent intermediate, with one-oxidizing equivalent resided in the ferryl state of the iron as [Fe(IV)=O] (low spin, $S=1$) and the second localized as a porphyrin π radical cation. Recently, a protein-centered radical has been detected, implicating that the second oxidizing equivalent may also localize on the Trp residue 172 near the heme prosthetic group with $S=1/2$ in., during the catalytic cycle of VP from *B. adusta* [203]. Electron paramagnetic resonance of H_2O_2-activated VP from *P. eryngii* shows that the surface Trp164 exists in the form of a neutral radical [201]. The oxidation of Mn(II) and aromatic substrates by direct electron transfer to the heme and long-range electron transfer from a surface accessible Trp residue is analogous to that observed in *P. chrysosporium* LiP, but the reactive form in the latter exists as a Trp radical cation [54, 202, 204]. Furthermore, hydroxylation of the Trp residue as found in the moiety of Trp171 in *P. chrysosporium* LiP-H8 has not been observed in the VP enzymes.

Chemical modification of Trp172 in the *B. adusta* enzyme significantly reduced Mn(II)-independent activity and decoloration of industrial dyes, while the Mn(II)-dependent activity was maintained [205]. Site-directed mutagenesis of the surface Trp164 to either Ser or His in the *P. eryngii* isozyme abolished completely the ability to oxidize both veratryl alcohol and reactive black 5, substrates typically used for LiP [200]. In both the cases of LiP and VP, the detection of a Trp radical translates into potentially the existence of an alternative form for compound I, which is characterized by two oxidizing equivalents located in the oxyferryl center, and in either the porphyrin ring radical cation or a Trp residue neutral radical [201, 203]. Multiple sites could be involved in oxidation of different aromatic substrates and dyes by these peroxidases [34].

The interconversion of structure/function between LiP and MnP is evidenced by a series of site-directed mutagenesis to introduce MnP activity to LiP or vice versa. A single mutation (Ser168 to Trp) of *P. chrysosporium* MnP H4 generates an enzyme hybrid capable of oxidizing a wide range of LiP substrates while retaining full Mn(II) oxidase activity [46]. The Ser168 in MnPH4 corresponds to surface Trp171 of LiP, which has been confirmed as the VA oxidation site and also critical for the broad substrate specificity [47]. In a reverse scheme, *P. chrysosporium* LiP H8 was engineered with a manganese-binding site, resulting in a mutant of combined catalytic properties of LiP and MnP [206]. The results from protein engineering therefore provide supporting evidence for the structural design of the natural enzyme hybrid.

Conclusion

The interest in utilizing ligninolytic enzymes for biotechnological applications has increased rapidly since the discovery of these enzymes in white-rot fungi. Emerging technologies include selective delignification for production of cellulosics in pulp bleaching, conversion of lignocelulosics into feed and biofuel, and treatment of environmental pollutants and toxicants generated in various industrial processes [207]. Lignin may represent a potential feedstock for the production of small molecular weight chemicals, such as vanillin, dimethyl sulfoxide, and phenols. While a great deal has been accomplished in understanding the major enzymes involved in lignin degradation, much remains to be explored. The structural properties of the peroxidases relating to the ability to

oxidize substrates of high redox potentials have not yet been thoroughly characterized. Further investigation is warranted on the precise role and the interactions of small molecule mediators in the catalytic mechanism of these enzymes as well as in the process of lignin degradation. Research on enzyme applications has shifted from focusing on a single enzyme preparation to selective combination of different enzymes or whole organisms. Despite recent progress, our understanding of the process has been hampered by substrate complexity and by the multiplicity of enzymes involved. Reconstitution of fungal ligninolytic systems with purified enzyme components has never reached the same level of efficiency. Most of the difficulties are due to the inability to isolate the native form of lignin encountered by fungi in nature. In addition, local environmental factors, such as temperature, moisture, pH, nitrogen, and oxygen levels exert critical influence on the ability of the fungus to degrade and utilize lignin. It is also clear now that lignin degradation involves not only the four major ligninolytic oxidases, but is a multi-enzymatic process with an array of accessory enzymes playing a cooperative role in a highly efficient manner. Elucidation of the role and interaction of enzyme combinations in lignin degradation are essential to providing a scientific base for the development of application technologies. The advent of DNA technology may provide a powerful tool for solving some of the challenges. In particular, the use of differential gene display and proteomic profiling may enable the detection of the global changes in the enzymes generated by the microorganism during lignin degradation. These approaches may provide a comprehensive picture of the physiological response of the microorganism at the biochemical and molecular level. They may also assist in exploring metabolic pathways specifically and allow access to the tremendous biotechnological potential of white-rot fungi.

References

1. Brunow, G. (2001). Methods to reveal the structure of lignin. In M. Hofrichter, & A. Steinbuchel (Eds.), *Lignin, humic substances and coal (Biopolymers, vol. 1)*. Weinheim, Germany: Wiley-VCH.
2. Fukushima, K. (2001). Regulation of syringyl to guaiacyl ratio in lignin biosynthesis. *Journal of Plant Research*, *114*, 499–508, doi:10.1007/PL00014017.
3. Higuchi, T. (2006). Look back over the studies of lignin biochemistry. *Journal of Wood Science*, *52*, 2–8, doi:10.1007/s10086-005-0790-z.
4. Del Rio, J. C., Marques, G., Rencoret, J., Martinez, A. T., & Gutierrez, A. (2007). Occurrence of naturally acetylated lignin units. *Journal of Agricultural and Food Chemistry*, *55*, 5461–5466, doi:10.1021/jf0705264.
5. Ralph, J., Lundquist, K., Brunow, G., Lu, F., Kim, H., Schatz, P. F., et al. (2004). Lignins: Natural polymers from oxidative coupling of 4-hydroxyphenylpropanoids. *Phytochemistry Review*, *3*, 29–60, doi:10.1023/B:PHYT.0000047809.65444.a4.
6. Alder, E. (1977). Lignin chemistry - past, present and future. *Wood Science and Technology*, *11*, 169–218, doi:10.1007/BF00365615.
7. Karhunen, P., Rummakko, P., Sipila, J., Brunow, G., & Kilpelainen, I. (1995). The formation of dibenzodiomocin structures by oxidative coupling. A model reaction for lignin biosynthesis. *Tetrahedron Letter*, *36*, 4501–4504, doi:10.1016/0040-4039(95)00769-9.
8. Argyropoulos, D. S., Jurasek, L., Kristofova, L., Xia, Z. C., Sun, Y. J., & Palus, E. (2002). Abundance and reactivity of dibenzodioxocins in softwood lignin. *Journal of Agricultural and Food Chemistry*, *50*, 658–666, doi:10.1021/jf010909g.
9. Zhang, L., & Gellerstedt, G. (2001). NMR observation of a new lignin structure, a spirodienone. *Chemical Communications*, 2744–2745.
10. Boerjan, W., Ralph, J., & Baucher, M. (2003). Lignin biosynthesis. *Annual Review Plant Biology*, *54*, 519–546, doi:10.1146/annurev.arplant.54.031902.134938.
11. Davin, L. B., & Lewis, N. G. (2003). A historical perspective on lignan biosynthesis: Monolignol, allylphenol and hydroxycinnamic acid coupling and downstream metabolism. *Phytochemistry Review*, *2*, 257–288, doi:10.1023/B:PHYT.0000046175.83729.b5.

12. Chen, Y.-R., & Sarkanen, S. (2003). Macromolecular lignin replication: A mechanistic working hypothesis. *Phytochemistry Review*, *2*, 235–255, doi:10.1023/B:PHYT.0000046173.38194.ba.
13. Brauns, F. E. (1939). Native lignin I. Its isolation and methylation. *Journal of the American Chemical Society*, *61*, 2120–2127, doi:10.1021/ja01877a043.
14. Buchanan, M. A., Brauns, F. E., & Leaf, Jr., R. L. (1949). Native lignin II. Native aspen lignin. *Journal of the American Chemical Society*, *71*, 1297–1299, doi:10.1021/ja01172a043.
15. Bjorkman, A. (1954). Isolation of lignin from finely divided wood with neutral solvents. *Nature*, *174*, 1057–1058, doi:10.1038/1741057a0.
16. Gellerstedt, G., Pranda, J., & Lindfors, E. L. (1994). Structural and molecular properties of residual birch kraft lignin. *Journal of Wood Chemistry and Technology*, *14*, 467–482, doi:10.1080/02773819408003108.
17. Alder, E., Pepper, J. M., & Eriksoo, E. (1957). Action of mineral acid on lignin and model substances of guaiacylglycerol-beta-aryl ether type. *Industrial Engineering Chemistry*, *49*, 1391–1392, doi:10.1021/ie50573a037.
18. Pew, J., & Weyna, P. (1962). Fine grinding, enzyme digestion and lignin-cellulose bond in wood. *TAPPI*, *45*, 247–256.
19. Chang, H. M., Cowling, E. B., Brown, W., Alder, E., & Miksche, G. (1975). Comparative studies on cellulolytic enzyme lignin and milled wood lignin of Sweetgum and Spruce. *Holzforschung*, *29*, 153–159.
20. Kirk, T. K., Connors, W. J., Bleam, R. D., Hackett, W. F., & Zeikus, J. G. (1975b). Preparation and microbial decomposition of synthetic [^{14}C]lignins. *Proceedings of the National Academy of Sciences of the USA*, *72*, 2515–2519, doi:10.1073/pnas.72.7.2515.
21. Kirk, T. K., & Brunow, G. (1988). Synthetic ^{14}C-labeled lignins. *Methods in Enzymology*, *161*, 65–73, doi:10.1016/0076-6879(88)61010-X.
22. Kirk, T. K., Connors, W. J., & Zeikus, G. (1976). Requirements for a growth substrate during lignin decomposition by two wood-rotting fungi. *Applied and Environmental Microbiology*, *32*, 192–194.
23. Mester, T., Varela, E., & Tien, M. (2004). *Wood degradation by brown-rot and white-rot fungi. The Mycota II: genetics and biotechnology (2nd edition)*. Springer-Verlag Berlin-Heidelberg.
24. Blanchette, R. A. (1984). Screening wood decayed by white rot fungi for preferential lignin degradation. *Applied and Environmental Microbiology*, *48*, 647–653, Medline.
25. Otjen, L., & Blanchette, R. (1987). Assessment of 30 white rot basidiomycetes for selective lignin degradation. *Holzforschung*, *41*, 343–349.
26. Blanchette, R. A. (1991). Delignification by wood-decay fungi. *Annual Review of Phytopathology*, *29*, 381–398, doi:10.1146/annurev.py.29.090191.002121.
27. Eriksson, K.-E. L., Blanchette, R. A., & Ander, P. (1990). *Microbial and Enzymatic Degradation of wood and wood components* p. 407. Berlin Heidelberg: Springer-Verlag.
28. Gilbertson, R. L. (1980). Wood-rotting fungi of north America. *Mycologia*, *72*, 1–49, doi:10.2307/3759417.
29. Cowling, E. B. (1961). Comparative biochemistry of decay of sweetgum sapwood by white-rot and brown-rot fungi. *USDA Technical Bulletin*, *1258*, 1–79.
30. Baldrian, P. (2005). Fungal laccases - occurrence and properties. *FEMS Microbiology Reviews*, *30*, 215–242, doi:10.1111/j.1574-4976.2005.00010.x.
31. Farrell, L. (1987). Combustion: The microbial degradation of lignin. *Annual Reviews in Microbiology*, *41*, 465–505, doi:10.1146/annurev.micro.41.1.465.
32. Gold, H. M., Youngs, H. L., & Sollewijn Gelpke, M. D. (2000). Manganese peroxidase. *Metal Ions in Biological Systems*, *37*, 559–586, Medline.
33. Kersten, P., & Cullen, D. (2007). Extracellular oxidative systems of the lignin-degrading Basidiomycete *Phanerochaete chrysosporium*. *Fungal Genetics Biology*, *44*, 77–87, doi:10.1016/j.fgb.2006.07.007.
34. Martinez, A. T. (2002). Molecular biology and structure-function of lignin-degrading heme peroxidases. *Enzyme Microbial Technology*, *30*, 425–444, doi:10.1016/S0141-0229(01)00521-X.
35. Martinez, A. T., Speranza, M., Ruiz-Duenas, F. J., Ferreira, P., Camarero, S., Guillen, F., et al. (2005). Biodegradation of lignocellulosics: microbial, chemical, and enzymatic aspects of the fungal attack of lignin. *International Microbiology*, *8*, 195–204, Medline.
36. Welinder, K. G. (1992). Superfamily of plant, fungal and bacterial peroxidases. *Current Opinion in Structural Biology*, *2*, 388–393, doi:10.1016/0959-440X(92)90230-5.
37. Tien, M., & Kirt, T. K. (1983). Lignin-degrading enzyme from the hymenomycetes *Phanerochaete chrysosporium* burds. *Science*, *221*, 661–663, doi:10.1126/science.221.4611.661.

38. Hammel, K. E., Jensen, Jr., K. A., Mozuch, M. D., Landucci, L. L., Tien, M., & Pease, E. A. (1993). Ligninolysis by a purified lignin peroxidase. *Journal of Biological Chemistry*, *268*, 12274–12281, Medline.
39. Valli, K., Wariishi, H., & Gold, M. H. (1990). Oxidation of monomethoxylated aromatic compounds by lignin peroxidase: Role of veratryl alcohol in lignin biodegradation. *Biochemistry*, *29*, 8535–8539, doi:10.1021/bi00489a005.
40. Edwards, S. L., Raag, R., Wariishi, H., Gold, M. H., & Poulos, T. L. (1993). Crystal structure of lignin peroxidase. *Proceedings of the National Academy of Sciences of the USA*, *90*, 750–754, doi:10.1073/pnas.90.2.750.
41. Poulos, T. L., Edwards, S. L., Wariishi, H., & Gold, M. H. (1993). Crystallographic refinement of lignin peroxidase at 2Δ. *Journal of Biological Chemistry*, *268*, 4429–4440, Medline.
42. Blodig, W., Smith, A. T., Doyle, W. A., & Piontek, K. (2001). Crystal structures of pristine and oxidatively processed lignin peroxidase expressed in *Escherichia coli* and of the W171F variant that eliminate the redox active tryptophan 171. Implications for the reaction mechanism. *Journal of Molecular Biology*, *305*, 851–861, doi:10.1006/jmbi.2000.4346.
43. Choinowski, T., Blodig, W., Winterhalter, K. H., & Piontek, K. (1999). The crystal structure of lignin peroxidase at 1.70Δ resolution reveals a hydroxy group on the C_β of tryptophan 171: A novel radical site formed during the redox cycle. *Journal of Molecular Biology*, *286*, 809–827, doi:10.1006/jmbi.1998.2507.
44. Blodig, W., Doyle, W. A., Smith, A. T., Winterhalter, K., Choinowski, T., & Piontek, K. (1998). Autocatalytic formation of a hydroxy group at the C_β of Trp171 in lignin peroxidase. *Biochemistry*, *37*, 8832–8838, doi:10.1021/bi9727186.
45. Doyle, W. A., Blodig, W., Weitch, N. C., Piontek, K., & Smith, A. T. (1998). Two substrate interaction sites in lignin peroxidase revealed by site-directed mutangesis. *Biochemistry*, *37*, 15097–15105, doi:10.1021/bi981633h.
46. Timofeevski, S. L., Nie, G., Reading, S., & Aust, S. D. (1999). Addition of veratryl alcohol oxidase activity to manganese peroxidase by site-directed mutagenesis. *Biochemical and Biophysical Research Communications*, *256*, 500–504, doi:10.1006/bbrc.1999.0360.
47. Timofeevski, S. L., Nie, G., Reading, S., & Aust, S. D. (2000). Substrate specificity of lignin peroxidase and a S168W variant of manganese peroxidase. *Archives of Biochemistry and Biophysics*, *373*, 147–153, doi:10.1006/abbi.1999.1562.
48. Wong, D. W. S. (1995). *Food enzymes: structure and mechanism* pp. 321–345. NY: Chapman & Hall.
49. Renganathan, V., & Gold, M. H. (1986). Spectral characterization of the oxidized states of lignin peroxidase, an extracellular heme enzyme from the white rot Basidiomycete *Phanerochaete chrysosporium*. *Biochemistry*, *25*, 1626–1631, doi:10.1021/bi00355a027.
50. Andrawis, A., Johnson, K. A., & Tien, M. (1988). Studies on Compound I formation of the lignin peroxidase from *Phanerochaete chrysosporium*. *Journal of Biological Chemistry*, *263*, 1196–1198.
51. Marquez, L., Wariishi, H., Dunford, H. B., & Gold, M. H. (1988). Spectroscopic and kinetic properties of the oxidized intermediates of lignin peroxidase from *Phanerochaete chrysosporium*. *Journal of Biological Chemistry*, *263*, 10549–10552, Medline.
52. Behere, D. V., Gonzalez-Vergara, E., & Goff, H. M. (1985). Unique cyanide nitrogen-15 nuclear magnetic resonance chemical shift values for cyano-eroxidase complexes. Relevance to the heme active-site structure and mechanism of peroxide activation. *Biochimica et Biophysica Acta*, *832*, 319–325.
53. Chance, B., Power, L., Ching, Y., Poulos, T., Schonbaum, G. R., Yamazaki, I., & Paul, K. G. (1984). X-Ray absorption studies of intermediates in peroxidase activity. *Archives of Biochemistry and Biophysics*, *235*, 596–611, doi:10.1016/0003-9861(84)90234-0.
54. Blodig, W., Smith, A. T., Winterhalter, K., & Piontek, K. (1999). Evidence from spin-trapping for a transient radical on tryptophan residue 171 of lignin peroxidase. *Archives of Biochemistry and Biophysics*, *370*, 86–92, doi:10.1006/abbi.1999.1365.
55. Tien, M., Kirk, T. K., Bull, C., & Fee, J. A. (1986). Steady-state and transient-state kinetic studies on the oxidation of 3,4-dimethoxybenzyl alcohol catalyzed by the ligninase of *Phanerocheate chrysosporium* Burds. *Journal of Biological Chemistry*, *261*, 1687–1683, Medline.
56. Ator, M. A., & de Montelano, P. R. O. (1987). Protein control of prosthetic heme activity. Reaction of substrates with the heme edge of horseradish peroxidase. *Journal of Biological Chemistry*, *262*, 1542–1551, Medline.
57. Schoemaker, H. E., & Piontek, K. (1996). On the interaction of lignin peroxidase with lignin. *Pure and Applied Chemistry*, *68*, 2089–2096, doi:10.1351/pac199668112089.

58. Sollewijn Gelpke, M. D., Lee, J., & Gold, M. H. (2002). Lignin peroxidase oxidation of veratryl alcohol: Effects of the mutants H82A, Q222A, W171A, and F267L. *Biochemistry*, *41*, 3498–3506, doi:10.1021/bi011930d.
59. Johjima, T., Wariishi, H., & Tanaka, H. (2002). Veratryl alcohol binding sites of lignin peroxidase from *Phanerochaete chrysosporium*. *Journal of Molecular Catalysis. B, Enzymatic*, *17*, 49–57.
60. Gerini, M. F., Roccatano, D., Baciocchi, E., & Nola, A. D. (2003). Molecular dynamics simulations of lignin peroxidase in solution. *Biophysical Journal*, *84*, 3883–3893.
61. Wariishi, H., & Gold, M. H. (1989). Lignin peroxidase compound III. Formation, inactivation, and conversion to the native enzyme. *FEBS Letters*, *243*, 165–168, doi:10.1016/0014-5793(89)80122-X.
62. Cai, D., & Tien, M. (1992). Kinetic studies on the formation and decomposition of compounds II and III. *Journal of Biological Chemistry*, *267*, 1149–1155.
63. Barr, D. P., & Aust, S. D. (1994). Conversion of lignin peroxidase compound III to active enzyme by cation radicals. *Archives of Biochemistry and Biophysics*, *312*, 511–515, doi:10.1006/abbi.1994.1339.
64. Schoemaker, H. E., Harvey, P. J., Bowen, R. M., & Palmer, J. M. (1985). On the mechanism of enzymatic lignin breakdown. *FEBS Letters*, *183*, 7–12, doi:10.1016/0014-5793(85)80942-X.
65. Baciocchi, E., Gerini, M. F., Lanzalunga, O., Lapi, A., Piparo, M. G. L., & Mancinelli, S. (2001a). Isotope-effect profiles in the oxidative *N*-demethylation of *N,N*-dimethylanilines catalyzed by lignin peroxidase and a chemical model. *European Journal of Organ Chemistry*, *2001*, 2305–2310, doi:10.1002/1099-0690(200106)2001:12<2305::AID-EJOC2305>3.0.CO;2-E.
66. Harvey, P. J., & Palmer, J. M. (1990). Oxidation of phenolic compounds by ligninase. *Journal of Biotechnology*, *13*, 169–179, doi:10.1016/0168-1656(90)90102-H.
67. Tien, M., & Kirk, T. K. (1984). Lignin-degrading enzyme from *Phanerochaete chrysosporium*: Purification, characterization, and catalytic properties of a unique H_2O_2-requiring oxygenase. *Proceedings of the National Academy of Sciences of the USA*, *81*, 2280–2284, doi:10.1073/pnas.81.8.2280.
68. Harvey, G.-F., Gilardi, G.-F., Goble, M. L., & Palmer, J. M. (1993). Charge transfer reactions and feedback control of lignin peroxidase by phenolic compounds: Significance in lignin degradation. *Journal of Biotechnology*, *30*, 57–69, doi:10.1016/0168-1656(93)90027-K.
69. Koduri, R. S., & Tien, M. (1995). Oxidation of guaiacol by lignin peroxidase. *Journal of Biological Chemistry*, *270*, 22254–22258, doi:10.1074/jbc.270.38.22254.
70. Dodson, P. J., Evans, C. S., Harvey, P. J., & Palmer, J. M. (1987). Production and properties of an extracellular peroxidase from *Corilus versicolor* which catalyzes $C_\alpha - C_\beta$ cleavage in a lignin model compound. *FEMS Microbiology Letter*, *42*, 17–22.
71. Chung, N., & Aust, S. D. (1995). Inactivation of lignin peroxidase by hydrogen peroxide during the oxidation of phenols. *Archives of Biochemistry and Biophysics*, *316*, 851–855, doi:10.1006/abbi.1995.1114.
72. Banci, L., Ciofi-Baffoni, S., & Tien, M. (1999). Lignin and Mn peroxidase-catalyzed oxidation of phenolic lignin oligomers. *Biochemistry*, *38*, 3205–3210, doi:10.1021/bi982139g.
73. Renganathan, V., Miki, K., & Gold, M. H. (1985). Multiple molecular forms of diarylpropane oxygenase, an H_2O_2-requiring, lignin-degrading enzyme from *Phanerochate chrysosporium*. *Archives of Biochemistry and Biophysics*, *241*, 304–314, doi:10.1016/0003-9861(85)90387-X.
74. Hammel, K. E., Tien, M., Kalyanaraman, B., & Kirk, T. K. (1985). Mechanism of oxidative $C_\alpha - C_\beta$ cleavage of a lignin model dimer by *Phanerochaete chrysosporium* ligninase. *Journal of Biological Chemistry*, *260*, 8348–8353.
75. Kirk, T. K., Tien, M., Kersten, P. J., & Mozuch, M. D. (1986). Ligninase of *Phanerochaete chrysosporium*. *Biochemistry Journal*, *236*, 279–287.
76. Miki, K., Renganathan, V., & Gold, M. H. (1986). Mechanism of β-aryl ether dimeric lignin model compound oxidation by lignin peroxidase of *Phanerochaete chrysosporium*. *Biochemistry*, *25*, 4790–4796, doi:10.1021/bi00365a011.
77. Miki, K., Kondo, R., Renganathan, V., Mayfield, M. B., & Gold, M. H. (1988). Mechanism of aromatic ring cleavage of a β-biphenylyl ether dimer catalyzed by lignin peroxidase of *Phanerochaete chrysosporium*. *Biochemistry*, *27*, 4787–4794, doi:10.1021/bi00413a031.
78. Umezawa, T., & Higuchi, T. (1989). Cleavages of aromatic ring and β-*O*-4 bond of synthetic lignin (DHP) by lignin peroxidase. *FEB Letter*, *242*, 325–329, doi:10.1016/0014-5793(89)80494-6.
79. Kersten, P. J., Tien, M., Kalyanaraman, B., & Kirk, T. K. (1985). The ligninase of *Phanerochaete chrysosporium* generates cation radicals from methoxybenzenes. *Journal of Biological Chemistry*, *260*, 2609–2612.
80. Baciocchi, E., Bietti, M., Gerini, M. F., Lanzalunga, O., & Mancinelli, S. (2001b). Oxidation of non-phenolic β-*O*-aryl-lignin model dimers catalyzed by lignin peroxidase. Comparison with the oxidation induced by potassium 12-tungstocobalt(III)ate. *Journal of the Chemical Society, 41*, 1506–1511, doi:10.1039/b101362i, Perkin Trans 2.

81. Lundell, T., Wever, R., Floris, R., Harvey, P., Hatakka, A., Brunow, G., et al. (1993). Lignin peroxidase L3 from *Phlebia radiata*. Pre-steady-state and steady-state studies with veratryl alcohol and a non-phenolic lignin model compound 1-(3,4-dimethoxyphenyl)-2-(2-methoxyphenoxy) propane-1,3-diol. *European Journal of Biochemistry*, *211*, 391–402, doi:10.1111/j.1432-1033.1993.tb17562.x.
82. Harvey, P. J., Schoemaker, H. E., Bowen, R. M., & Palmer, J. M. (1985). Single-electron transfer processes and the reaction mechanism of enzymic degradation of lignin. *FEBS Letters*, *183*, 13–16, doi:10.1016/0014-5793(85)80943-1.
83. Wariishi, H., Huang, J., Dunford, B., & Gold, M. H. (1991). Reactions of lignin compounds I and II with veratryl alcohol. *Journal of Biological Chemistry*, *266*, 20694–20699.
84. Walling, C., El-Talwi, G. M., & Amarnalth, K. (1984). Oxidation of styrene derivatives by S2O8 2– CuII in acetic acid and acetonitrile. Reaction paths in oxidations via radical cations. *Journal of the American Chemical Society*, *106*, 7373–7578, doi:10.1021/ja00336a043.
85. Fenn, P., & Kirk, T. K. (1981). Relationship of nitrogen to the onset and suppression of ligninolytic activity and secondary metabolism in *Phanerochaete chrysosporium*. *Archives of Microbiology*, *130*, 59–65, doi:10.1007/BF00527073.
86. Faison, B. D., & Kirk, T. K. (1985). Factors involved in the regulation of ligninase activity in *Phanerochaete chrysosporium*. *Applied and Environmental Microbiology*, *49*, 299–304.
87. Schoemaker, H. E., & Leisola, M. S. A. (1990). Degradation of lignin by *Phanerochaete chrysosporium*. *Journal of Biotechnology*, *13*, 101–109, doi:10.1016/0168-1656(90)90096-T.
88. Bietti, M., Baciocchi, E., & Steenken, S. (1998). Lifetime, reduction potential and base-induced fragmentation of the veratryl alcohol radical cation in aqueous solution. Pulse radiolysis studies on a ligninase "mediator". *Journal of Physical Chemistry A*, *102*, 7337–7342, doi:10.1021/jp9812482.
89. Harvey, P. J., Schomaker, H. E., & Palmer, J. M. (1986). Veratryl alcohol as a mediator and the role of radical cations in lignin biodegradation by *Phanerochaete chrysosporium*. *FEBS Letters*, *195*, 242–246, doi:10.1016/0014-5793(86)80168-5.
90. Khindaria, A., Grover, T. A., & Aust, S. D. (1995). Evidence for formation of the veratryl alcohol cation radical by lignin peroxidase. *Biochemistry*, *34*, 6020–6025, doi:10.1021/bi00018a003.
91. Khindaria, A., Nie, G., & Aust, S. D. (1997). Detection and characterization of the lignin peroxidase compound II - veratryl alcohol cation radical complex. *Biochemistry*, *36*, 14181–14185 doi:10.1021/bi9715730.
92. Baciocchi, E., Bietti, M., Gerini, M. F., & Lanzalunga, O. (2002). The mediation of veratryl alcohol in oxidations prompted by lignin peroxidase: the lifetime of veratryl alcohol radical cation. *Biochemistry and Biophysics Research Communications*, *293*, 832–835, doi:10.1016/S0006-291X(02)00306-6.
93. Schmidt, H. W. H., Haemmerli, S. D., Schoemaker, H. E., & Leisola, M. S. A. (1989). Oxidative degradation of 3,4-dimethoxybenzyl alcohol and its methyl ether by the lignin peroxidase of *Phanerochaete chrysosporium*. *Biochemistry*, *28*, 1776–1783, doi:10.1021/bi00430a053.
94. Haemmerli, S. D., Schoemaker, H. E., Schmidt, H. W. H., & Leisola, M. S. A. (1987). Oxidation of veratryl alcohol by the lignin peroxidase of *Phanerochaete chrysosporium*. Involvement of activated oxygen. *FEBS Letters*, *220*, 149–154, doi:10.1016/0014-5793(87)80893-1.
95. Have, R. T., & Franssen, M. C. R. (2001). On a revised mechanism of side product formation in the lignin peroxidase catalyzed oxidation of veratryl alcohol. *FEBS Letters*, *487*, 313–317 doi:10.1016/S0014-5793(00)02379-6.
96. Goodwin, D. C., Aust, S. D., & Grover, T. A. (1995). Evidence for veratryl alcohol as a redox mediator in lignin peroxidase-catalyzed oxidation. *Biochemistry*, *34*, 5060–5065, doi:10.1021/bi00015a017.
97. Tien, M., & Ma, D. (1997). Oxidation of 4-methoxymandelic acid by lignin peroxidase. *Journal of Biological Chemistry*, *272*, 8912–8917, doi:10.1074/jbc.272.14.8912.
98. Christian, V., Shrivastava, R., Shukla, D., Modi, H., & Vyas, B. R. M. (2005). Mediator role of veratryl alcohol in the lignin peroxidase-catalyzed oxidative decolorization of remazol brilliant blue R. *Enzyme Microbial Technology*, *36*, 426–431, doi:10.1016/j.enzmictec.2004.06.007.
99. Khindaria, A., Yamazaki, I., & Aust, S. D. (1996). Stabilization of the veratryl alcohol cation radical by lignin peroxidase. *Biochemistry*, *35*, 6418–6424, doi:10.1021/bi9601666.
100. Baciocchi, E., Bietti, M., & Steenken, S. (1998). Lifetime, reduction potential and base-induced fragmentation of the veratryl alcohol radical cation in aqueous solution. Pulse radiolysis studies on a ligninase "mediator". *Journal of Physical Chemistry A*, *102*, 7337–7342, doi:10.1021/jp9812482.
101. Joshi, D. K., & Gold, M. H. (1996). Oxidation of dimethoxylated aromatic compounds by lignin peroxidase from *Phanerochaete chrysosporium*. *European Journal of Biochemistry*, *237*, 45–57, doi:10.1111/j.1432-1033.1996.0045n.x.

102. Kersten, P. J., Kalyanaraman, B., Hammel, K. E., & Reinhammar, B. (1990). Comparison of lignin peroxidase, horseradish peroxidase and laccase in the oxidation of methoxybenzene. *Biochemistry Journal*, *268*, 475–480.
103. Cui, F., & Dolphin, D. (1990). The role of manganese in model systems related to lignin biodegradation. *Holzforschung*, *44*, 279–283.
104. Reinhammar, B. R. M. (1972). Oxidation-reduction potentials of the electron acceptors in laccase and stellacyanin. *Biochimica et Biophysica Acta*, *275*, 245–259, doi:10.1016/0005-2728(72)90045-X.
105. Xu, F., Berka, R. M., Wahleithner, J. A., Nelson, B. A., Shuster, J. R., Brown, S. H., et al. (1998). Site-directed mutations in fungal laccase: effect on redox potential, activity and pH profile. *Biochemistry Journal*, *334*, 63–70.
106. Hayashi, Y., & Yamazaki, I. (1979). The oxidation-reduction potentials of compound I/compound II and compound II/ferric couples of horseradish peroxidase A2 and C. *Journal of Biological Chemistry*, *254*, 9101–9106.
107. Conroy, C. W., Tyma, P., Daum, P. H., & Erman, J. E. (1978). Oxidation-reduction potential measurements of cytochrome c peroxidase and pH dependent spectral transition in the ferrous enzyme. *Biochimica et Biophysica Acta*, *537*, 62–69.
108. Popp, J. L., & Kirk, T. K. (1991). Oxidation of methoxybenzenes by manganese peroxidase and by Mn^{3+}. *Archives of Biochemistry and Biophysics*, *268*, 145–148, doi:10.1016/0003-9861(91)90176-J.
109. Bonnarme, P., & Jeffries, T. W. (1990). Mn(II) regulation of lignin peroxidases and manganese-dependent peroxidases from lignin-degrading white rot fungi. *Applied Environmental Microbiology*, *56*, 210–217.
110. Brown, J. A., Alic, M., & Gold, M. H. (1991). Manganese peroxidase gene transcription in *Phanerochaete chrysosporium*: Activation by manganese. *Journal of Bacteriology*, *173*, 4101–4106.
111. Gettemy, J. M., Ma, B., Alic, M., & Gold, M. H. (1998). Reverse transcription-PCR analysis of the regulation of the manganese peroxidase gene family. *Applied and Environmental Microbiology*, *64*, 569–574.
112. Alic, M., Akileswaran, L., & Gold, M. H. (1997). Characterization of the gene encoding manganese peroxidase isozyme 3 from *Phanerochaete chrysosporium*. *Biochimica et Biophysica Acta*, *1338*, 1–7.
113. Mester, T., & Field, J. A. (1997). Optimization of manganese peroxidase production by the white rot fungus *Bjerkandera* sp. strain BOS55. *FEMS Microbiology Letter*, *155*, 161–168, doi:10.1111/j.1574-6968.1997.tb13873.x.
114. Mester, T., de Jong, E., & Field, J. A. (1995). Manganese regulation of veratryl alcohol in white rot fungi and its indirect effect on lignin peroxidase. *Applied and Environmental Microbiology*, *61*, 1881–1887.
115. Pease, E. A., & Tien, M. (1992). Heterogeneity and regulation of manganese peroxidases from *Phanerochaete chrysosporium*. *Journal of Bacteriology*, *174*, 3532–3540.
116. Glenn, J. K., & Gold, M. H. (1985). Purification and characterization of an extracellular Mn(II)-dependent peroxidase from the lignin-degrading Basidiomycete, *Phanerochaete chrysosporium*. *Archives of Biochemistry and Biophysics*, *242*, 329–341, doi:10.1016/0003-9861(85)90217-6.
117. Mino, Y., Wariishi, H., Blackburn, N. J., Loehr, T. M., & Gold, M. H. (1988). Spectral characterization of manganese peroxidase, an extracellular heme enzyme from the lignin-degrading basidiomycete, *Phanerochaete chrysosporium*. *Journal of Biological Chemistry*, *263*, 7029–7036.
118. Sundaramoorthy, M., Kishi, K., Gold, M. H., & Poulos, T. L. (1994). The crystal structure of manganese peroxidase from *Phanerochaete chrysosporium* at 2.06-Δ resolution. *Journal of Biological Chemistry*, *269*, 32759–32767.
119. Sundaramoorthy, M., Kishi, K., Gold, M. H., & Poulos, T. L. (1997). Crystal structure of substrate binding site mutants of manganese peroxidase. *Journal of Biological Chemistry*, *272*, 17574–17580, doi:10.1074/jbc.272.28.17574.
120. Sundaramoorthy, M., Youngs, H. L., Gold, M. H., & Poulos, T. L. (2005). High-resolution crystal structure of manganese peroxidase: Substrate and inhibitor complexes. *Biochemistry*, *44*, 6463–6470, doi:10.1021/bi047318e.
121. Glenn, J. K., Akileswaran, L., & Gold, M. H. (1986). Mn(II) oxidation is the principal function of the extracellular Mn-peroxidase from *Phanerochaete chrysosporium*. *Archives of Biochemistry and Biophysics*, *251*, 688–696, doi:10.1016/0003-9861(86)90378-4.
122. Paszczynski, A., Huynh, V. -B., & Crawford R. (1986). Comparison of ligninase-I and peroxidase-M2 from the white-rot fungus *Phanerochaete chrysosporium*. *244*, 750–765.
123. Wariishi, H., Dunford, H. B., MacDonald, I. D., & Gold, M. H. (1989a). Manganese peroxidase from the lignin-degrading Basidiomycete *Phanerochaete chrysosporium*. Transient state kinetics and reaction mechanism. *Journal of Biological Chemistry*, *264*, 3335–3340.
124. Wariishi, H., Akileswaran, L., & Gold, M. H. (1988). Manganese peroxidase from the Basidiomycete *Phanerochaete chrysosporium*: Spectral characterization of the oxidized states and the catalytic cycle. *Biochemistry*, *27*, 5365–5370, doi:10.1021/bi00414a061.

125. Wariishi, H., Valli, K., & Gold, M. H. (1992). Manganese(II) oxidation by manganese peroxidase from the Basidiomycete *Phanerochaete chrysosporium*. *Journal of Biological Chemistry*, *267*, 23688–23695.
126. Kishi, K., Wariishi, H., Marquez, L., Dunford, H. B., & Gold, M. H. (1994). Mechanism of manganese peroxidase compound II reduction. Effect of organic acid chelators and pH. *Biochemistry*, *33*, 8694–8701, doi:10.1021/bi00195a010.
127. Kuan, I.-C., Johnson, K. A., & Tien, M. (1993). Kinetic analysis of manganese peroxidase. *Journal of Biological Chemistry*, *268*, 20064–20070.
128. Zapanta, L. S., & Tien, M. (1997). The roles of veratryl alcohol and oxalate in fungal lignin degradation. *Journal of Biotechnology*, *53*, 93–102, doi:10.1016/S0168-1656(96)01678-1.
129. Khindaria, A., Grover, T. A., & Aust, S. D. (1994). Oxalate-dependent reductive activity of manganese peroxidase from *Phanerochaete chrysosporium*. *Archives of Biochemistry and Biophysics*, *314*, 301–306, doi:10.1006/abbi.1994.1446.
130. Urzua, U., Kersten, P. J., & Vicuna, R. (1998). Manganese peroxidase-dependent oxidation of glyoxylic and oxalic acids synthesized by *Ceriporiopsis subvermispora* produces extracellular hydrogen peroxide. *Applied and Environmental Microbiology*, *64*, 68–73.
131. Wariishi, H., Valli, K., Renganathan, V., & Gold, M. H. (1989b). Oxidative cleavage of a phenolic diarylpropane lignin model dimer by manganese peroxidase from *Phanerochaete chrysosporium*. *Biochemistry*, *28*, 6017–6023, doi:10.1021/bi00440a044.
132. Tuor, U., Wariishi, H., Schoemaker, H. E., & Gold, M. H. (1992). Oxidation of phenolic aryglycerol β-aryl ether lignin model compounds by manganese peroxidase from *Phanerochaete chrysosporium*: Oxidative cleavage of an α-carbonyl model compound. *Biochemistry*, *31*, 4986–4995, doi:10.1021/bi00136a011.
133. Reddy, G. V. B., Sridhar, M., & Gold, M. H. (2003). Cleavage of nonphenolic β-1 diarylpropane lignin model dimers by manganese peroxidase from *Phanerochaete chrysosporium*. *European Journal of Biochemistry*, *270*, 284–292, doi:10.1046/j.1432-1033.2003.03386.x.
134. Wariishi, H., Valli, K., Renganathan, V., & Gold, M. H. (1989c). Thiol-mediated oxidation of nonphenolic lignin model compounds by manganese peroxidase of *Phanerochaete chrysosporium*. *Journal of Biological Chemistry*, *264*, 14185–14191.
135. Bao, W., Fukushima, Y., Jensen, K. A., Moen, M. A., & Hammel, K. E. (1994). Oxidative degradation of non-phenolic lignin during lipid peroxidation by fungal manganese peroxidase. *FEBS Letters*, *354*, 297–300, doi:10.1016/0014-5793(94)01146-X.
136. Daina, S., Orlandi, M., Bestetti, G., Wiik, C., & Elegir, G. (2002). Degradation of β-5 lignin model dimers by *Ceriporiopsis subvermispora*. *Enzyme Microbial Technology*, *30*, 499–505, doi:10.1016/S0141-0229(01)00524-5.
137. Kapich, A., Hofrichter, M., Vares, T., & Hatakka, V. (1999). Coupling of manganese peroxidase-mediated lipid peroxidation with destruction of nonphenolic lignin model compounds and ^{14}C-labeled lignins. *Biochemical and Biophysical Research Communications*, *259*, 212–219, doi:10.1006/bbrc.1999.0742.
138. Kapich, A. N., Steffen, K. T., Hofrichter, M., & Hatakka, A. (2005). Involvement of lipid oxidation in the degradation of a non-phenolic lignin model compound by manganese peroxidase of the litter-decomposing fungus *Stropharia coronilla*. *Biochemical and Biophysical Research Communications*, *330*, 371–377, doi:10.1016/j.bbrc.2005.02.167.
139. Wariishi, H., & Gold, M. H. (1990). Lignin peroxidase compound III. Mechanism of formation and decomposition. *Journal of Biological Chemistry*, *265*, 2070–2077.
140. Timofeevski, S. L., Reading, N. S., & Aust, S. D. (1998). Mechanisms for protection against inactivation of manganese peroxidase by hydrogen peroxide. *Archives of Biochemistry and Biophysics*, *356*, 287–295, doi:10.1006/abbi.1998.0776.
141. Yoshida, H. (1883). Chemistry of lacquer (urushi). *Journal of the Chemical Society*, *43*, 472–486.
142. Givaudan, A., Effosse, A., Faure, D., Potier, P., Bouillant, M.-L., & Bally, R. (1993). Polyphenol oxidase in *Azospirillum lipoferum* isolated from rice rhizosphere: Evidence for laccase activity in non-motile strains of *Azospirillum lipoferum*. *FEMS Microbiology Letter*, *108*, 205–210, doi:10.1111/j.1574-6968.1993.tb06100.x.
143. Suzuki, T., Endo, K., Ito, M., Tsujibo, H., Miyamoto, K., & Inamori, Y. (2003). A thermostable laccase from *Streptomyces lavendulae* REN-7: Purification, characterization, nucleotide sequence, and expression. *Bioscience, Biotechnology, and Biochemistry*, *67*, 2167–2175, doi:10.1271/bbb.67.2167.
144. Hullo, M.-F., Moszer, I., Danchin, A., & Martin-Verstraete, I. (2001). CotA of *Bacillus subtilis* is a copper-dependent laccase. *Journal of Bacteriology*, *183*, 5426–5430, doi:10.1128/JB.183.18.5426-5430.2001.
145. Marco, A. E., & Roubelakis-Angelakis, K. A. (1997). Laccase activity could contribute to cell-wall reconstitution in regenerating protoplasts. *Phytochemistry*, *46*, 421–425, doi:10.1016/S0031-9422(97)00301-4.

146. Bao, W., O'Malley, D. M., Whetten, R., & Sederoff, R. R. (1993). A laccase associated with lignification in Loblolly pine xylem. *Science*, 672–674, doi:10.1126/science.260.5108.672.
147. Sterjiades, R., Dean, J. F. D., Gamble, G., Himmelsbach, D. S., & Eriksson, K. -E. L. (1993). Extracellular laccases and peroxidases from sycamore mapple (*Acer psudoplatanus*) cell-suspension cultures. *Planta*, *190*, 75–87, doi:10.1007/BF00195678.
148. Leatham, G. F., & Stahmann, M. A. (1981). Studies on the laccase of *Lentinus edodes*: specificity, localization and association with the development of fruiting bodies. *Journal of General Microbiology*, *125*, 147–157.
149. Youn, H.-D., Hah, Y. C., & Kang, S.-O. (1995). Role of laccase in lignin degradation by white-rot fungi. *FEMS Microbiology Letter*, *132*, 183–188, doi:10.1111/j.1574-6968.1995.tb07831.x.
150. Eggert, C., Temp, U., & Eriksson, K. -E. L. (1997). Laccase is essential for lignin degradation by the white-rot fungus *Pycnoporus cinnabarinus*. *FEBS Letters*, *407*, 89–92, doi:10.1016/S0014-5793(97)00301-3.
151. Thurston, C. F. (1994). The structure and function of fungal laccases. *Microbiology*, *140*, 19–26.
152. Bertrand, T., Jolivalt, C., Briozzo, P., Caminade, E., Joly, N., Madzak, C., et al. (2002). Crystal structure of a four-copper laccase complex with an arylamine: Insights into substrate recognition and correlation with kinetics. *Biochemistry*, *41*, 7325–7333, doi:10.1021/bi0201318.
153. Ducros, V., Brzozowski, A. M., Wilson, K. S., Brown, S. H., Ostergaard, P., Schneider, P., et al. (1998). Crystal structure of the type-2 Cu depleted laccase from Coprinus cinereus at 2.2Δ resolution. *Nature Structural Biology*, *5*, 310–316, doi:10.1038/nsb0498-310.
154. Piontek, K., Antorini, M., & Choinowski, T. (2002). Crystal structure of a laccase from the fungus *Trametes versicolor* at 1.90-Δ resolution containing a full complement of coppers. *Journal of Biological Chemistry*, *277*, 37663–37669, doi:10.1074/jbc.M204571200.
155. Hakulinen, N., Kiiskinen, L.-L., Kruus, K., Saloheimo, M., Paananen, A., Koivula, A., et al. (2002). Crystal structure of a laccase of *Melanocarpus albomyces* with an intact trinuclear copper site. *Nature Structural Biology*, *9*, 601–605.
156. Antorini, M., Herpoel-Gimbert, I., Choinowski, T., Sigoillot, J.-C., Asther, M., Winterhalter, K., et al. (2002). Purification, crystallization and X-ray diffraction study of fully functional laccases from two ligninolytic fungi. *Biochimica et Biophysica Acta*, *1594*, 109–114.
157. Garavaglia, S., Cambria, M. T., Miglio, M., Ragusa, S., Lacobazzi, V., Palmieri, F., et al. (2004). The structure of *Rigidoporus lignosus* laccase containing a full component of copper ions, reveals an asymmetrical arrangement for the T3 copper pair. *Journal of Molecular Biology*, *342*, 1519–1531, doi:10.1016/j.jmb.2004.07.100.
158. Enguita, F. J., Martins, L. O., Henriquest, A. O., & Carrondo, M. A. (2003). Crystal structure of a bacterial endospore coat component. A laccase with enhanced thermostability properties. *Journal of Biological Chemistry*, *278*, 19416–19425, doi:10.1074/jbc.M301251200.
159. Malkin, R., & Malmstrom, B. G. (1970). The state and function of copper in biological systems. *Advance Enzymology*, *33*, 177.
160. Dooley, D. M., Rawlings, J., Dawson, J. H., Stephens, P. J., Andreasson, L.-E., Malmstrom, B. C., et al. (1979). Spectroscopic studies of *Rhus vernicifera* and *Polyporus versicolor* laccase. Electronic structures of the copper sites. *Journal of the American Chemical Society*, *101*, 5038–5046, doi:10.1021/ja00511a039.
161. Palmer, A. E., Randall, D. W., Xu, F., & Solomon, E. I. (1999). Spectroscopic studies and electronic structure description of the high potential type 1 copper site in fungal laccase: Insight into the effect of the axial ligand. *Journal of the American Chemical Society*, *121*, 7138–7149, doi:10.1021/ja991087v.
162. Reinhammar, B. R. M., & Vanngard, T. I. (1971). The electron-accepting sites in *Rhus vernicifera laccase* as studied by anaerobic oxidation-reduction titrations. *European Journal of Biochemistry*, *18*, 463–468, doi:10.1111/j.1432-1033.1971.tb01264.x.
163. Xu, F., Shin, W., Brown, S. H., Wahleithner, J. A., Sundaram, U. M., & Solomon, E. I. (1996). A study of a series of recombinant fungal laccases and bilirubin oxidase that exhibit significant differences in redox potential, substrate specificity, and stability. *Biochimica et Biophysica Acta*, *1292*, 303–311.
164. Xu, F. (1996). Oxidation of phenols, anilines, and benzenethiols by fungal laccases: Correlation between activity and redox potentials as well as halide inhibition. *Biochemistry*, *35*, 7608–7614, doi:10.1021/bi952971a.
165. Messerschmidt, A., Ladenstein, R., Huber, R., Bolognesi, M., Avigliano, L., Petruzzelli, R., et al. (1992). Refined crystal structure of ascorbate oxidase at 1.9Δ resolution. *Journal of Molecular Biology*, *224*, 179–205, doi:10.1016/0022-2836(92)90583-6.
166. Zoppellaro, G., Sakurai, T., & Huang, H.-W. (2001). A novel mixed valence form of *Rhus vernicifera* laccase and its reaction with dioxygen to give a peroxide intermediate bound to the trinuclear center. *Journal of Biochemistry*, *129*, 949–953.

167. Huang, H.-W., Zopellaro, G., & Sakurai, T. (1999). Spectroscopic and kinetic studies on the oxygen-centered radical formed during the four-electron reduction process of dioxygen by *Rhus vernicifera* laccase. *Journal of Biological Chemistry*, *274*, 32718–32724, doi:10.1074/jbc.274.46.32718.
168. Palmer, A. E., Lee, S. K., & Solomon, E. I. (2001). Decay of the peroxide intermediate in laccase: Reductive cleavage of the O-O bond. *Journal of the American Chemical Society*, *123*, 6591–6599, doi:10.1021/ja010365z.
169. Lee, S.-K., George, S. D., Antholine, W. E., Hedman, B., Hodgson, K. O., & Solomon, E. I. (2002). Nature of the intermediate formed in the reduction of O_2 to H_2O at the trinuclear copper cluster active site in native laccase. *Journal of the American Chemical Society*, *124*, 6180–6193, doi:10.1021/ja0114052.
170. Zoppellaro, G., Huang, H.-W., & Sakurai, T. (2000). Kinetic studies on the reaction of the fully reduced laccase with dioxygen. *Inorganic Reaction Mechanisms*, *2*, 79–84.
171. Lundquist, K., & Kristersson, P. (1985). Exhaustive laccase-catalyzed oxidation of a lignin model compound (vanillyl glycol) produces methanol and polymeric quinoid products. *Biochemistry Journal*, *259*, 277–279.
172. Kawai, S., Umezawa, T., & Higuchi, T. (1999a). Degradation mechanisms of phenolic β-1 lignin substructure model compounds by laccase of *Coriolus versicolor*. *Archives of Biochemistry and Biophysics*, *262*, 99–110, doi:10.1016/0003-9861(88)90172-5.
173. Faure, D., Bouillant, M. L., Jacoud, C., & Bally, R. (1996). Phenolic derivatives related to lignin metabolism as substrates for *Azospirillum laccase* activity. *Phytochemistry*, *42*, 357–359, doi:10.1016/0031-9422(95)00869-1.
174. Kawai, S., Umezawa, T., Shimada, M., & Higuchi, T. (1999b). Aromatic ring cleavage of 4,6-di(*tert*) guaiacol, a phenolic lignin model compound, by laccause of *Coriolus versicolor*. *FEBS Letters*, *236*, 309–311, doi:10.1016/0014-5793(88)80043-7.
175. Bourbonnais, R., & Paice, M. G. (1990). Oxidation of non-phenolic substrates. An expanded role for laccase in lignin biodegradation. *267*, 99–102.
176. Bourbonnais, R., Paice, M. G., Freiermuth, B., Bodie, E., & Borneman, S. (1997). Reactivities of various mediators and laccases with kraft pulp and lignin model compounds. *Applied and Environmental Microbiology*, *63*, 4627–4632.
177. Eggert, C., Temp, U., Dean, J. F. D., & Eriksson, K.-E. L. (1996). A fungal metabolite mediates degradation of non-phenolic lignin structures and synthetic lignin by laccase. *FEBS Letters*, *391*, 144–148, doi:10.1016/0014-5793(96)00719-3.
178. Fabbrini, M., Galli, C., & Gentili, P. (2002). Comparing the catalytic efficiency of some mediators of laccase. *Journal of Molecular Catalysis. B, Enzymatic*, *16*, 231–240, doi:10.1016/S1381-1177(01)00067-4.
179. Baiocco, P., Barreca, A. M., Fabbrini, M., Galli, C., & Gentili, P. (2003). Promoting laccase activity towards non-phenolic substrates: a mechanistic investigation with some laccase-mediator systems. *Organ Biomolecular Chemistry*, *1*, 191–197, doi:10.1039/b208951c.
180. Bourbonnais, R., Leech, D., & Paice, M. G. (1998). Electrochemical analysis of the interactions of laccase mediators with lignin model compounds. *Biochimica et Biophysica Acta*, *1379*, 381–390.
181. Claus, H., Faber, G., & Konig, H. (2002). Redox-mediated decolorization of synthetic dyes by fungal laccases. *Applied Microbiology and Biotechnology*, *59*, 672–678, doi:10.1007/s00253-002-1047-z.
182. Gutierrez, A., del Rio, J. C., Ibarra, D., Rencoret, J., Romero, J., Speranza, M., et al. (2006a). Enzymatic removal of free and conjugated sterols forming pitch deposits in environmentally sound bleaching of eucalypt paper pulp. *Environmental Science & Technology*, *40*, 3416–3422, doi:10.1021/es052547p.
183. Gutierrez, A., del Rio, J. C., Rencoret, J., Ibarra, D., & Martinez, A. T. (2006b). Main liphilic extractives in different paper pulp tpes can be removed using the laccase-mediator system. *Applied Microbiology and Biotechnology*, *72*, 845–851, doi:10.1007/s00253-006-0346-1.
184. Gutierrez, A., Rencoret, J., Ibarra, D., Molina, S., Camareo, S., Romero, J., et al. (2007). Removal of lipophilic extractives from paper by laccase and lignin-derived phenols as natural mediators. *Environmental Science & Technology*, *41*, 4124–4129, doi:10.1021/es062723+.
185. Kawai, S., Nakagawa, M., & Ohashi, H. (2002). Degradation mechanisms of nonphenolic β-*O*-4 lignin model dimer by *Trametes versicolor* laccase in the presence of 1-hydroxybenzotriazole. *Enzyme Microbial Technology*, *30*, 482–489, doi:10.1016/S0141-0229(01)00523-3.
186. Kawai, S., Iwatsuki, M., Nakagawa, M., Inagaki, M., Hamabe, A., & Ohashi, H. (2004). An alternative β-ether cleavage pathway for a non-phenolic β-*O*-4 lignin model dimer catalyzed by a laccase-mediator system. *Enzyme Microbial Technology*, *35*, 154–160, doi:10.1016/j.enzmictec.2004.03.019.
187. Li, K., Xu, F., & Eriksson, K.-E. L. (1999). Comparison of fungal laccases and redox mediators in oxidation of a nonphenolic lignin model compound. *Applied and Environmental Microbiology*, *65*, 2654–2660.
188. Hirai, H., Shibata, H., Kawai, S., & Nishida, T. (2006). Role of 1-hydroxybenzotriazole in oxidation by laccase from *Trametes versicolor*. Kinetic analysis of the laccase-1-hydroxybenzotriazole couple. *FEMS Microbiology Letter*, *265*, 56–59, doi:10.1111/j.1574-6968.2006.00474.x.

189. Mester, T., & Field, J. A. (1998). Characterization of a novel manganese peroxidase-lignin peroxidase hybrid isozyme produced by *Bjerkandera* species strain BOS55 in the absence of manganese. *Journal of Biological Chemistry*, 15412–15417, doi:10.1074/jbc.273.25.15412.
190. Moreira, P., Duez, G., Dehareng, D., Antunes, A., Almeida-Vara, E., Frere, J. M., et al. (2005). Molecular characterization of a versatile peroxidase from a *Bjerkandera* strain. *Journal of Biotechnology*, *118*, 339–352, doi:10.1016/j.jbiotec.2005.05.014.
191. Martinez, M., Ruiz-Duenas, F. J., Guillen, F., & Martinez, A. T. (1996). Purification and catalytic properties of two manganese peroxidase isoenzymes from *Pleurotus eryngii*. *European Journal of Biochemistry*, *237*, 424–432, doi:10.1111/j.1432-1033.1996.0424k.x.
192. Heinfling, A., Ruiz-Duenas, F. J., Martinez, M. J., Berbauer, M., Szewzyk, U., & Martinez, A. T. (1998). A study on reducing substrates of manganese-oxidizing peroxidases from *Pleurotus eryngii* and *Bjerkandera adusta*. *FEBS Letters*, *428*, 141–146, doi:10.1016/S0014-5793(98)00512-2.
193. Wang, Y., Vazquez-Duhalt, R., & Pickard, M. A. (2003). Manganese-lignin peroxidase hybride from *Bjerkandera adusta* oxidizes polycyclic aromatic hydrocarbons more actively in the absence of manganese. *49*, 675–682.
194. Camarero, S., Bockle, B., Martinez, M. J., & Martinez, A. T. (1996). Manganese-mediated lignin degradation by *Pleurotus pulmonarius*. *Applied and Environmental Microbiology*, *62*, 1070–1072.
195. Camarero, S., Sarkar, S., Ruiz-Duenas, F. J., Martinez, M. J., & Martinez, A. T. (1999). Description of a versatile peroxidase involved in the natural degradation of lignin that has been manganese peroxidase and lignin peroxidase substrate interaction sites. *Journal of Biological Chemistry*, *274*, 10324–10330, doi:10.1074/jbc.274.15.10324.
196. Kamitsuji, H., Honda, Y., Watanabe, T., & Kuwahara, M. (2005). Mn^{2+} is dispensable for the production of active MnP2 by *Pleurotus ostreatus*. *Biochemistry Biophysics Research Communication*, *327*, 871–876, doi:10.1016/j.bbrc.2004.12.084.
197. Rodakiewicz-Nowak, J., Jarosz-Wilkolazka, A., & Luterek, J. (2006). Catalytic activity of versatile peroxidase from *Bjerkandera fumosa* in aqueous solutions of water-miscible organic solvents. *Applied Catalysis A: General*, *308*, 56–61, doi:10.1016/j.apcata.2006.04.009.
198. Ruiz-Duenas, F. J., Martinez, M. J., & Martinez, A. T. (1999). Molecular characterization of a novel peroxidase isolated from the ligninolytic fungus *Pleurotus eryngii*. *Molecular Microbiology*, *31*, 223–235, doi:10.1046/j.1365-2958.1999.01164.x.
199. Ruiz-Duenas, F. J., Morales, M., Perez-Boada, M., Choinowski, T., Martinez, M. J., Piontek, K., et al. (2007). Manganese oxidation site in *Pleurotus eryngii* versatile peroxidase: A site-directed mutagenesis, kinetic, and crystallographic study. *Biochemistry*, *46*, 66–77, doi:10.1021/bi061542h.
200. Perez-Boada, M., Ruiz-Duenas, F. J., Pogni, R., Basosi, R., Choinowski, T., Martinez, M., et al. (2005). Versatile peoxidase oxidation of high redox potential aromatic compounds: Site-directed mutagenesis, spectroscopic and crystallographic investigation of three long-range electron transfer pathways. *Journal of Molecular Biology*, *354*, 385–402, doi:10.1016/j.jmb.2005.09.047.
201. Pongi, R., Camilla Baratto, M., Teutloff, C., Giansanti, S., Ruiz-Duenas, F. J., Choinowski, T., et al. (2006). A tryptophan neutral radical in the oxidized state of versatile peroxidase from *Pleurotus eryngii*. *Journal of Biological Chemistry*, *281*, 9517–9526.
202. Johjima, T., Itoh, H., Kabuto, M., Tokimura, F., Nakagawa, T., Wariishi, H., et al. (1999). Direct interaction of lignin and lignin peroxidase from *Phanerochaete chrysosporium*. *Proceedings of the National Academy of Sciences of the USA*, *96*, 1989–1994, doi:10.1073/pnas.96.5.1989.
203. Pogni, R., Camilla Baratto, M., Giansanti, S., Teutloff, C., Verdin, J., Valderrama, B., et al. (2005). Tryptophan-based radical in the catalytic mechanism of versatile peroxidase from *Bjerkandera adusta*. *Biochemistry*, *44*, 4267–4274, doi:10.1021/bi047474l.
204. Camarero, S., Ruiz-Duenas, J., Sarkar, S., Martinez, M. J., & Martinez, A. T. (2000). The cloning of a new peroxidase found in lignocellulose cultures of *Pleurotus eryngii* and sequence comparison with other fungal peroxidases. *FEMS Microbiology Letter*, *191*, 37–43, doi:10.1111/j.1574-6968.2000.tb09316.x.
205. Tinoco, R., Verdin, J., & Vazquez-Duhalt, R. (2007). Role of oxidizing mediators and tryptophan 172 in the decoloration of industrial dyes by the versatile peroxidases from *Bjerkandera adusta*. *Journal of Molecular Catalysis. B, Enzymatic*, *46*, 1–7, doi:10.1016/j.molcatb.2007.01.006.
206. Mester, T., & Tien, M. (2001). Engineering of a manganese-binding site in lignin peroxidase isozyme H8 from *Phanerochaete chrysosporium*. *Biochemical and Biophysical Research Communications*, *284*, 723–728, doi:10.1006/bbrc.2001.5015.
207. Mester, T., & Tien, M. (2000). Oxidation mechanism of ligninolytic enzymes involved in the degradation of environmental pollutants. *International Biodeterioration & Biodegradation*, *46*, 51–59, doi:10.1016/S0964-8305(00)00071-8.